

Complex interplay between organic and secondary inorganic aerosols with ambient relative humidity implicates the aerosol liquid water content over India during wintertime

Amar Krishna Gopinath¹, Subha S Raj¹, Snehitha Kommula¹, Christi Jose¹, Upasana Panda², Yukti Bhishambu¹, Narendra Ojha³, Ravikrishna R¹, Pengfei Liu⁴, and Sachin S Gunthe⁵

¹Indian Institute of Technology Madras

²CSIR Institute of Minerals and Materials Technology

³Physical Research Laboratory (PRL)

⁴School of Earth and Atmospheric Sciences, Georgia Institute of Technology

⁵Environmental and Water Resources Engineering Division, Department of Civil Engineering, Indian Institute of Technology Madras, Chennai 600036, India.

November 22, 2022

Abstract

Aerosol Liquid Water Content (ALWC), a ubiquitous component of atmospheric aerosols, contributes to total aerosol mass burden, modulating atmospheric chemistry through aerosol surface reactions and reducing atmospheric visibility. However, the complex dependency of ALWC on aerosol chemistry and relative humidity (RH) in the Indian region remains poorly characterized. Here, we combine available measurements of aerosol chemical composition with thermodynamic model ISORROPIA2.1 to reveal a comprehensive picture of ALWC in fine mode aerosols during the winter season in the Indian region. The factors modulating ALWC are primarily dependent on the RH, such that the effect of aerosol dry mass and hygroscopicity are significant at high RH while the effect of hygroscopicity loses its significance as RH is lowered. ALWC, depending upon the particle hygroscopicity, displays a sharp non-linear rise beyond a critical value of ambient RH. Further analysis coupling WRF-Chem simulation with ISORROPIA2.1 revealed significant spatial heterogeneity in ALWC over India, strongly associating with regions of high aerosol loading and RH. The Indo-Gangetic Plain is consequently observed to be a hotspot of higher ALWC, which explains the prevalent conditions of haze and smog during winter in the region. Our findings re-emphasize that high aerosol mass resulting from intense pollution is vital in modulating aerosol-climate interaction under favorable meteorological conditions. They suggest the need for pollution control strategies to be directed at the reduction in emissions of specific species like NH₃ and NO_x, which were observed to contribute to the enhancement of PM and ALWC during wintertime in the region.

Complex interplay between organic and secondary inorganic aerosols with ambient relative humidity implicates the aerosol liquid water content over India during wintertime

Amar Krishna Gopinath^{1,2}, Subha S. Raj^{2,3}, Snehitha M. Kommula^{2,3}, Christi Jose^{2,3}, Upasana Panda^{2,3,4}, Yukti Bishambu^{2,3}, Narendra Ojha⁵, R. Ravikrishna^{1,2}, Pengfei Liu⁶, Sachin S. Gunthe^{2,3}

¹Department of Chemical Engineering, Indian Institute of Technology Madras, Chennai, India

²Laboratory for Atmospheric and Climate Sciences, Indian Institute of Technology Madras, Chennai, India

³EWRE Division, Department of Civil Engineering, Indian Institute of Technology Madras, Chennai, India

⁴Academy of Scientific and Innovative Research (AcSIR), Department of Environment and Sustainability, CSIR – Institute of Minerals and Materials Technology, Bhubaneswar, India

⁵Space and Atmospheric Sciences Division, Physical Research Laboratory, Ahmedabad 380 009, India

⁶School of Earth and Atmospheric Sciences, Georgia Institute of Technology, Atlanta, GA, USA

Key Points:

- Aerosol Liquid Water Content (ALWC) is ubiquitous in atmospheric aerosols in the Indian region during winter.
- ALWC is enhanced drastically at high aerosol loading at high relative humidity.
- Reduction of NH₃ and NO_x emissions is re-emphasised for pollution reduction and visibility improvement in the Indo-Gangetic Plain.

Corresponding author: Pengfei Liu, pengfei.liu@eas.gatech.edu

Corresponding author: Sachin S. Gunthe, s.gunthe@iitm.ac.in

Abstract

Aerosol Liquid Water Content (ALWC), a ubiquitous component of atmospheric aerosols, contributes to total aerosol mass burden, modulating atmospheric chemistry through aerosol surface reactions and reducing atmospheric visibility. However, the complex dependency of ALWC on aerosol chemistry and relative humidity (RH) in the Indian region remains poorly characterized. Here, we combine available measurements of aerosol chemical composition with thermodynamic model ISORROPIA2.1 to reveal a comprehensive picture of ALWC in fine mode aerosols during the winter season in the Indian region. The factors modulating ALWC are primarily dependent on the RH, such that the effect of aerosol dry mass and hygroscopicity are significant at high RH while the effect of hygroscopicity loses its significance as RH is lowered. ALWC, depending upon the particle hygroscopicity, displays a sharp non-linear rise beyond a critical value of ambient RH. Further analysis coupling WRF-Chem simulation with ISORROPIA2.1 revealed significant spatial heterogeneity in ALWC over India, strongly associating with regions of high aerosol loading and RH. The Indo-Gangetic Plain is consequently observed to be a hotspot of higher ALWC, which explains the prevalent conditions of haze and smog during winter in the region. Our findings re-emphasize that high aerosol mass resulting from intense pollution is vital in modulating aerosol–climate interaction under favourable meteorological conditions. They suggest the need for pollution control strategies to be directed at the reduction in emissions of specific species like NH_3 and NO_x , which were observed to contribute to the enhancement of PM and ALWC during wintertime in the region.

Plain Language Summary

Water vapour condenses on particulates in the air (known as atmospheric aerosols) due to the presence of chemical species with high water affinity. The condensed water, referred to as Aerosol Liquid Water Content (ALWC), is primarily responsible for weather conditions of low visibility like haze and smog, which have impacts on human health, and economy. This study has calculated ALWC using existing measurement data of the chemical composition of fine sized aerosols from literature, for contrasting and diverse environments in India. The study has focused on the winter season marked by spike in pollution levels and haze. Relative humidity, total particle concentration, and chemical composition were identified to play a significant role in influencing ALWC. The Indo-Gangetic Plain has been identified to be a hotspot of high ALWC due to high pollution levels and relative humidity particularly during winter season. The need for reduction of the levels of NH_3 in the atmosphere originating from agricultural waste and NO_3^- originating from motor emissions are suggested, as the primary focus for the reduction of atmospheric pollution and ALWC for improving visibility over the region.

1 Introduction

Aerosol Liquid Water Content (ALWC) is a significant component of atmospheric aerosols that affects their size, lifetime, and chemical properties. The presence of ALWC is primarily due to the absorption of water vapour by the chemical species that constitute aerosols (Seinfeld & Pandis, 2016). Water uptake occurs drastically when aerosols are subjected to ambient relative humidity (RH) greater than critical values known as deliquescence RH (DRH) for single component particles and mutual deliquescence RH (MDRH) for multicomponent particles (Wexler & Seinfeld, 1991; Zaveri et al., 2005). Upon reduction of ambient RH below DRH or MDRH, aerosols may not, however, lose the condensed water to undergo phase transition into solid state. Experimental studies suggest a hysteresis phenomenon wherein ALWC is observed to exist even when ambient RH is much lower than the DRH or MDRH (Tang et al., 1995; Tang & Fung, 1997). Such a metastable state has been observed in ambient aerosols in various field studies (Rood et al., 1987, 1989). This observation not only suggests the ubiquity of ALWC, but also

signifies its effect on physical and chemical properties of aerosols for a wide range of RH. High ambient RH facilitates the growth of aerosols by water uptake, leading to enhanced surface area for heterogeneous reactions, higher aqueous phase reaction rates and uptake coefficients of trace acidic gases (Hennigan et al., 2008; Cheng et al., 2016; Faust et al., 2017; Song et al., 2019; Y. Wang et al., 2020; Kommula et al., 2021). Therefore, ALWC serves as a medium for chemical reactions, especially at high RH. The subsequent secondary formation of highly hygroscopic species leads to further water uptake, causing a positive feedback effect on the formation of aerosols (Huang et al., 2014; G. Wang et al., 2016; Cheng et al., 2016; Z. Wu et al., 2018). ALWC may also modulate the aerosol pH and possibly affect atmospheric chemistry under conditions of strong ammonia emissions (Zheng et al., 2020). ALWC substantially modifies the optical properties of aerosols by increasing their extinction coefficient, consequently enhancing the Aerosol Optical Depth (AOD) (Dougle et al., 1996; Sequeira & Lai, 1998). Moreover, high ALWC leads to poor visibility in the form of haze and smog over highly polluted locations (Dall’Osto et al., 2009; Chen et al., 2012; Gunthe et al., 2021). These effects ultimately modify the planetary albedo and radiative forcing, thereby perturbing the Earth’s energy balance (Dougle et al., 1996; Adams et al., 2001; Liao & Seinfeld, 2005).

The water uptake by aerosols mainly depends on the particulate mass burden, aerosol number concentration, size distribution, composition of gas and aerosol phase, RH, and temperature (Petters & Kreidenweis, 2007; Bian et al., 2014; Nguyen et al., 2016; Kuang et al., 2018). The gradient of water activity between aerosol particles and their surroundings is the major driving force for ALWC and hence, ambient RH being a proxy for the activity of water vapour in the atmosphere under sub-saturated conditions is a significant parameter (Seinfeld & Pandis, 2016). Hence, higher the RH level in the atmosphere, greater is the driving force for water uptake by aerosols (P. F. Liu et al., 2011; Bian et al., 2014; Z. Wu et al., 2018; Shen et al., 2019). Aerosol hygroscopicity, a measure of the water affinity of aerosol particles, is primarily a function of chemical composition in the particulate phase. The composition of atmospheric aerosols is, however, complex, ranging from inorganic species of high hygroscopicity to insoluble soot and a myriad of organic products, leading to varying levels of particle hygroscopicity in diverse environments. At high RH and low temperature, secondary formation of aerosols and their growth through heterogeneous gas to particle reactions are favoured, which may considerably alter the particulate chemical composition (Y. Wang et al., 2020; Cheng et al., 2016; Faust et al., 2017; P. F. Liu et al., 2011; Kommula et al., 2021). Chemical composition also varies with the size of aerosols, further adding to the complexity of aerosol hygroscopicity (Deshmukh et al., 2016; Boreddy et al., 2021; S. Kumar et al., 2018).

Real time measurement of ALWC in ambient aerosols has not been feasible yet due to technical limitations (Kuang et al., 2018). Hence, ALWC is generally measured indirectly by experimental techniques which usually involve the measurement of the difference in volume of aerosols at low and high RH. The difference is then used to calculate the aerosol growth factor (GF) (Bian et al., 2014; Fajardo et al., 2016; Kuang et al., 2018; Jin et al., 2020). A more common method is the estimation of ALWC using thermodynamic models, based on the assumption of thermodynamic equilibrium within the particle phase and between the particle and surrounding gaseous phases. Numerous models based on thermodynamic equilibrium have been reported in literature including EQUIL, MARS, AIM, SCAPE, EQUISOLV, ISORROPIA etc. (Bassett & Seinfeld, 1983; P. Saxena et al., 1986; Wexler & Seinfeld, 1991; Kim et al., 1993; Jacobson et al., 1996; Nenes et al., 1998; Wexler & Clegg, 2002), which mostly consider the aerosol chemistry pertaining to the inorganic species only. Nguyen et al. (2016) estimated ALWC using the model ISORROPIA2.1 based on AMS chemical composition measurements from various locations around the world, providing a good overview of the prevalence of ALWC. The study had not, however, examined the diverse and contrasting environments in the Indian region. Model estimates of ALWC have shown appreciable correlation to measured values in numerous closure studies (Bian et al., 2014; Fajardo et al., 2016; Kuang et al., 2018; Shen et al., 2019; Jin et al., 2020). Combining observations from experimen-

tal and modelling data, hygroscopicity of individual inorganic and organic compounds have also been parameterized in various studies (H. J. Liu et al., 2014; Petters & Kreidenweis, 2007).

The Indian region continues to experience severe air pollution, with many of its cities among the most polluted areas in the world (D. Ghosh & Parida, 2015). Modelling studies have identified an increasing trend in the aerosol loading across the Indian region with significant seasonal variability (Krishna Moorthy et al., 2013; Babu et al., 2013). Such high aerosol loading has been associated with severe health consequences such as respiratory-cardiovascular diseases and premature mortality (Lelieveld et al., 2015; Conibear et al., 2018; David et al., 2019; Guttikunda & Goel, 2013; Balakrishnan et al., 2018; Pandey et al., 2021). Moreover, poor visibility caused by the consequent haze and smog has had economic implications in the region by disturbing surface-air transport and day to day activities (Kulkarni et al., 2019). Although numerous studies have measured fine mode particulate matter and their chemical composition using online and offline techniques to address their air quality and public health impacts (Rastogi et al., 2016; Deshmukh et al., 2016; Rengarajan et al., 2011; S. Kumar et al., 2018; A. Kumar & Sarin, 2010; Agarwal et al., 2020; Jain et al., 2021; Gani et al., 2019; Thamban et al., 2019; Mukherjee et al., 2018; Kompalli et al., 2020; Ajith et al., 2022; Gunthe et al., 2021; Kommula et al., 2021), fewer studies have focused on the analysis of ALWC in this region (Boreddy et al., 2021; Satsangi et al., 2021; Kommula et al., 2021; Acharja et al., 2022). The winter season, particularly over the continental part of India, is marked by high atmospheric stability due to weak winds and temperature inversion, leading to poor dispersion of polluted air masses (Satsangi et al., 2021; Rastogi et al., 2016; M. Saxena et al., 2017; S. Raj et al., 2021). Studies have observed pronounced diurnal variations of RH and temperature during winter which causes strong radiative thermal inversions resulting in a shallow nocturnal planetary boundary layer (PBL) (S. Raj et al., 2021; Arun et al., 2018; Murthy et al., 2020). The stagnation and accumulation of aerosol emissions complemented by such favourable meteorological conditions enhance secondary aerosol mass, further aggravating the aerosol loading (Rastogi et al., 2016; Satsangi et al., 2021). Secondary aerosol formation results from the oxidation reaction of acidic gases SO_2 , NO_x and HCl with NH_3 emissions, leading to the nucleation and growth of highly hygroscopic inorganic species and also by nucleation and condensation of organic aerosols from the atmospheric oxidation of volatile organic compounds (VOC) (Satsangi et al., 2021; Deshmukh et al., 2016; Singh & Kulshrestha, 2012). These atmospheric processes consequently lead to widespread occurrences of haze and smog, especially in the Indo Gangetic Plain (IGP) region (Kumari et al., 2021; Satsangi et al., 2021; Gunthe et al., 2021; Ram & Sarin, 2011).

Thus, measurement of particulate matter and their chemical characterisation needs to be complemented by an adequate understanding of the characteristics of ALWC at varied conditions of RH. In this work, a comprehensive analysis is performed to understand the dependence of the water uptake and hygroscopic characteristics of atmospheric aerosols on their concentration, chemical composition and ambient RH. ALWC is estimated from chemical composition measurements of fine mode aerosols from ten diverse locations in India using thermodynamic modelling, focusing on the winter season. The data under consideration is characterised by different measurement techniques, measurement periods and environmental conditions and has been subsequently analysed with the necessary caution. The analysis is expected to provide a general and broad understanding of the factors governing ALWC over the Indian region, a key knowledge gap that is being addressed through this study.

2 Methodology

2.1 Analysis of chemical composition data and other considerations

To derive the distribution of aerosol liquid water content (ALWC) across India during wintertime, the average chemical composition of ambient aerosols at different locations was documented from various field campaign data reported in literature. Since the present study focuses only on the fine mode ambient aerosols, the chemical composition data of PM_{1.0} aerosols measured using spectrometric techniques as well as that of PM_{2.5} aerosols measured using filter based techniques were collected. The spectrometric methods used to measure PM_{1.0} include the Aerosol Mass Spectrometer (AMS) and Aerosol Chemical Speciation Monitor (ACSM). The measured data consists of mass concentrations of inorganic ions - sulphate (SO_4^{2-}), nitrate (NO_3^-), ammonium (NH_4^+), chloride (Cl^-), and organic matter. These instruments do not measure the concentration of refractory chemical species, which are mostly of sea salt or dust origin (Canagaratna et al., 2007; Nuaaman et al., 2015; Schlag et al., 2016; Zhang et al., 2017). The locations with ACSM/AMS based aerosol chemical composition data considered in this analysis include New Delhi (Gani et al., 2019), Kanpur (Thamban et al., 2019), Chennai (Kommula et al., 2021), Mahabaleshwar (Mukherjee et al., 2018), Bhubhaneshwar (Kompalli et al., 2020), and Thiruvananthapuram (Ajith et al., 2022). These locations not only represent diverse environmental conditions but also those which are meteorologically distinct even during the same seasons.

The filter based data set comprises of the mass concentration of only inorganic ions - sulphate (SO_4^{2-}), nitrate (NO_3^-), ammonium (NH_4^+), chloride (Cl^-), sodium (Na^+), calcium (Ca^{2+}), magnesium (Mg^{2+}) and potassium (K^+). Organic matter may be estimated from available filter-based Organic Carbon (OC) measurements. Though, the chemical composition measurements are generally in terms of ionic concentrations, the chemical species in the aerosols are generally found to be salt species with associations between the cations and anions. While the anionic species measured by the filter method may be associated with any of the cationic species, the anionic species measured by ACSM/AMS are associated only with NH_4^+ . This is because ACSM and AMS are only sensitive to non refractory salts like $(\text{NH}_4)_2\text{SO}_4$, NH_4NO_3 and NH_4Cl (among inorganic salts), which are ionisable at 600°C - the temperature of the in-built vaporiser used in the instruments (Canagaratna et al., 2007; Nuaaman et al., 2015). Ionic balance between cations and anions may be ideally used to separate the anionic species associated with only NH_4^+ in the filter data, so as to ensure compatibility with the ACSM/AMS data set. The ion pairing scheme by Gysel et al. (2007) is a commonly used method for ion balance but it is limited to only NH_4^+ , SO_4^{2-} and NO_3^- ions. Alastuey et al. (2005) and Mirante et al. (2014) have suggested a comprehensive ion balance methodology incorporating all other major ionic species also. However, considerable uncertainty is associated with the concentration of certain ionic species in the present data as the ion balance may not be sufficiently accurate to be generalised for the diverse environmental conditions under consideration. For example, Cl^- depletion at marine locations results in uncertainty regarding the sea salt origin of the measured Cl^- (Sarin et al., 2011; Kaushik et al., 2021). In the case of thermodynamic models, ion balance performed within the models are based on the assumption that the aerosols are internally mixed (Fountoukis & Nenes, 2007) while in reality, ambient aerosols may be externally mixed from different sources. Hence, these models may not accurately predict the cation-anion associations among ions of diverse origins like sea salt spray, dust re-suspension or emissions from combustion of fuels. For instance, thermodynamic models have predicted CaSO_4 in the aerosol, based on filter measurements of chemical composition at locations with high concentration of Ca^{2+} (Lin et al., 2013, 2014; Tao et al., 2014). Prediction of insoluble CaSO_4 may be inconsistent with the fact that the measured ionic species used as input to the models were water soluble, due to the nature of the filter technique used. Hence, predictions based on filter based

data by aerosol chemistry models require caution, especially when the measured aerosols are known to be externally mixed.

Thus, owing to the limitations mentioned above, in this study, only those locations have been chosen where the cationic composition is NH_4^+ dominant, so that it is conclusive that the measured anions are dominantly associated with NH_4^+ . Based on this assumption, only SO_4^{2-} , NO_3^- , NH_4^+ and Cl^- concentrations were considered from the filter data set to have the uniform comparison with ACSM/AMS data set. Field studies have reported the dominance of these ionic species in fine mode aerosols during wintertime in the Indian region, compared to summer and monsoon (M. Sharma et al., 2007; Rastogi et al., 2016; Agarwal et al., 2020). These species are mainly dominated by secondary particle formation from their precursor gases, enabled by high ambient RH, low temperature and atmospheric stability during wintertime (Singh & Kulshrestha, 2012; M. Saxena et al., 2017; Ram et al., 2010; Stockwell et al., 2000; Chutia et al., 2019). Studies have reported NH_4^+ to be the most dominant cation to correlate with the anionic species during the winter season (Rengarajan et al., 2011; Rastogi et al., 2016; Deshmukh et al., 2016; Agarwal et al., 2020). Furthermore, the Indian region generally experiences winds from continental locations during wintertime (Deshmukh et al., 2016; P. Kumar & Yadav, 2016; S. Kumar et al., 2018; Agarwal et al., 2020; A. Kumar et al., 2020; A. Ghosh et al., 2021; Jain et al., 2021), enriched in precursor gases which are the products of crop residue burning and industrial emissions (Deshmukh et al., 2016; Rastogi et al., 2016; Agarwal et al., 2020). Pollutant enriched atmosphere complemented by favourable meteorological conditions have been observed to result in high loading of secondary species in the region during winter (Ojha et al., 2020). These reasons explain the observed dominance of NH_4^+ in the chemical composition and enable us to exclude other cations from the analysis without significant loss of accuracy of the nominal prediction of ALWC. Coastal locations with filter data were also excluded, where effects like chloride depletion are prominent. For continental locations which are being considered in this study, winds from the coasts are dominant only during the monsoon season (P. Kumar & Yadav, 2016; A. Kumar et al., 2020), thus implying minimal influence of sea salt aerosols in these regions during winter. For a quantitative representation of the assumptions, the dominance of NH_4^+ was expressed in terms of the fraction of NH_4^+ among cations on equivalent molar basis, which essentially represents the contribution of NH_4^+ relative to all cations in neutralising the anions. Only those locations with fraction greater than 0.7 were chosen for the analysis, as shown in Table S1. The molar ratio $\text{NH}_4^+/\text{SO}_4^{2-} \geq 1.5$ has also been used to infer complete neutralisation of SO_4^{2-} by NH_4^+ as described in various studies (Agarwal et al., 2020; Satsangi et al., 2021; Pathak et al., 2009) and has been calculated and tabulated in Table S1 for the data under consideration.

Apart from these species, the concentration of potassium (K^+) is also listed from the filter data for additional analyses. The locations where filter based data are available include Patiala (Rastogi et al., 2016), Ahmedabad (Rengarajan et al., 2011), Bhopal (S. Kumar & Raman, 2016; Samiksha et al., 2021) and Amritsar (S. Kumar et al., 2018). Few locations with data on only inorganic ion concentrations and no OC (organic carbon) concentration, such as Mount Abu (A. Kumar & Sarin, 2010), Sikandarpur (Agarwal et al., 2020) and Patna (A. Kumar et al., 2020) are also included for additional analyses. The collected chemical composition data for the winter months is averaged over the respective campaign periods and shown in Table S1. Since the ACSM/AMS and filter based data correspond to different aerosol size ranges ($\text{PM}_{1.0}$ and $\text{PM}_{2.5}$ respectively), the data sets would be separately analysed without any inter-comparison for the scope of uniformity.

The lack of organics concentration in the filter based data needed to be compensated since organics have a significant influence on the overall hygroscopicity of ambient aerosols. Organic matter could be significantly composed of water soluble species, which are generally labelled as water soluble organic carbon (WSOC), formed from ox-

idation of VOCs or ageing of primary organic aerosol emissions (Faust et al., 2017). WSOC ratio has been reported to be high in the IGP region in India (Ram et al., 2010). In fact, earlier studies have estimated significantly high hygroscopicity for organic matter, which meant that they could have an enhancing effect on the overall water uptake characteristics of ambient aerosols (Cruz & Pandis, 2000; Jin et al., 2020; Fajardo et al., 2016; Engelhart et al., 2011). Studies have also shown that water contributed by organic matter could be significant as an enabler for secondary aerosol formation reactions (Jin et al., 2020). Thus, in this study, Organic Matter (OM) was estimated for the filter based locations using the Organic Carbon (OC) data by multiplying a mass conversion factor to the OC mass concentration as suggested in literature (Patel & Rastogi, 2018; Rastogi et al., 2016).

$$\text{Organic Matter} = \text{Mass factor} \times \text{Organic Carbon} \quad (1)$$

Mass conversion factor is the ratio of an estimated molecular weight of OM to the molecular weight of carbon and is determined based on the type of location. A mass conversion factor of 1.6 and 1.9 is recommended in literature for urban and aged aerosols respectively (Turpin & Lim, 2001).

2.2 Thermodynamic modelling of ALWC

The ALWC prediction for all locations was determined using the thermodynamic model ISORROPIA2.1 based on the average aerosol chemical composition, RH, and temperature. The model considers only inorganic species (SO_4^{2-} , NO_3^- , NH_4^+ , Cl^- , Na^+ , Ca^{2+} , Mg^{2+} and K^+) in its calculations and does not account for presence of any organic matter (Fountoukis & Nenes, 2007) in the aerosols. ISORROPIA2.1 exhibits rapid and robust convergence, with excellent performance with regard to computational speed, which makes it extremely suitable for incorporation into large-scale atmospheric transport and air quality models (Fountoukis & Nenes, 2007). Closure studies show that ALWC predictions made by ISORROPIA have agreed with growth factor based measurements for $\text{RH} > 60\%$ (Bian et al., 2014; Tan et al., 2017; Jin et al., 2020). Reported discrepancies were assumed to occur due to various reasons including the difficulty to model highly non ideal behaviour of concentrated aqueous phase of the aerosol at low RH (Wexler & Clegg, 2002) and lower number of species under consideration in the model, which could lead to errors in the estimated MDRH points (Bian et al., 2014).

Since the measured data consists of only particle phase concentrations and no gaseous phase concentrations, the analysis was performed in the reverse mode of ISORROPIA. The reverse mode assumes the total particle phase concentration as the basis for the model to predict the equilibrium gaseous phase concentrations based on gas-particle partitioning and distribution of chemical species in the solid and liquid phases within the particle. Calculations were performed in the metastable mode of ISORROPIA2.1. Observations on the phase state of ambient atmospheric aerosols have indicated the dominance of the metastable state, wherein the aerosols are expected to coexist in liquid state below their mutual deliquescence point (Rood et al., 1989; Tang et al., 1995; Tang & Fung, 1997). Aerosols have been observed to display hysteresis with respect to their phase state, in which water uptake occurs at DRH/MDRH and the transition back to a dry state occurs at a significantly lower critical RH known as the Efflorescence Relative Humidity (ERH) (Rood et al., 1987). Thus, observations of metastable state may be explained by the strong diurnal cycling of RH in the atmosphere (Shrestha et al., 2013).

ISORROPIA does not consider the aerosol curvature effects described by the Kelvin effect to be significant in its calculations (Nenes et al., 1998). The ambient vapour pressure of water is also considered to be unaffected by water uptake by the aerosols and hence, the water activity in any phase, under the assumptions of phase equilibrium between all three phases, is assumed to be the RH of ambient air, expressed on a scale ranging from 0.0 to 1.0.

$$(a_w) = RH \quad (2)$$

ISORROPIA calculates ALWC using the Zdanovskii Stokes Robinson (ZSR) correlation (Stokes & Robinson, 1966),

$$W = \sum \frac{M_i}{m_{oi}(a_w)} \quad (3)$$

where W is the mass concentration of the water taken up by the aerosol (kg m^{-3} air), M_i is the molar concentration of the i^{th} electrolyte (mol m^{-3} air), and $m_{oi}(a)$ is the molality of an aqueous binary solution of the i^{th} electrolyte with the same activity a_w as in the multicomponent solution. The ZSR rule describes the water uptake of internally mixed particles as the sum of the water uptake by the constituent chemical compounds.

The nature of organic species is generally complex that they may contribute positively or negatively to the aerosol hygroscopicity based on its chemical composition (P. Saxena et al., 1995; Cruz & Pandis, 2000). Despite this uncertainty, the contribution of organics to the ALWC was estimated by applying the κ -Kohler theory (Petters & Kreidenweis, 2007) with the ZSR mixing rule,

$$V_{w,org} = V_{d,org} \kappa_{org} \frac{a_w}{1 - a_w} \quad (4)$$

where $V_{w,org}$ is the ALWC corresponding to the organics, $V_{d,org}$ is the volume of the organics and κ_{org} is the hygroscopicity parameter corresponding to the organics and a_w is the water activity, which is assumed to be equal to the RH. $V_{d,org}$ is calculated by dividing the organic mass concentration by an assumed organic density of 1.4 g/cm^3 (Turpin & Lim, 2001; Jin et al., 2020). As discussed earlier, organic matter may have significant hygroscopicity as in the case of WSOC, for which κ was observed to be as high as 0.3 in several studies (Lambe et al., 2011; Massoli et al., 2010). Since WSOC has not been quantified for all locations under consideration in the respective measurement data, a nominal value of κ_{org} was assumed as recommended from literature, based on the type of location. κ_{org} was assumed to be 0.08 and 0.13 for urban and rural locations, respectively (Nguyen et al., 2016). The $V_{w,org}$ thus calculated was added to the ALWC predicted by ISORROPIA for the inorganics to obtain the total volume of ALWC, V_w .

2.3 Estimation of inorganic electrolytes

The ALWC predicted by the ZSR correlation (Equation 3) is based on the assumption that the total water content is the sum of contribution of various individual chemical compounds formed by the ionic species present in the aerosol, which has been validated by previous studies (Petters et al., 2009; Z. J. Wu et al., 2013). It is interesting to note that the correlation neglects any interactions occurring between these chemical compounds within the bulk of the aerosol particle (Moore & Raymond, 2008).

In order to analyse the inorganic compounds contributing to the predicted ALWC, the ion balance performed by ISORROPIA2.1 was determined by running the model in dry mode (Almeida et al., 2019; Tao et al., 2021). ISORROPIA2.1 predicts the salt species based on the relative concentration of NH_4^+ , Na^+ and crustal ion concentrations, parameterised as sulphate, sodium and crustal ratios (Fountoukis & Nenes, 2007). The mass concentration of salt species obtained from the model were used to calculate their individual contribution to ALWC using the ZSR correlation. The water uptake of a particular salt is the ratio of its molar concentration and binary molality as shown in Equation 3. The binary molalities of individual salts were determined using parametric data for the correlation between binary molality and activity obtained from literature (Fountoukis & Nenes, 2007; Pilinis & Seinfeld, 1987). The water uptake per unit mass of individual salt species were also calculated for a range of RH.

2.4 Estimation of hygroscopicity parameter κ

The hygroscopicity parameter κ is a single parameter representation for the particle hygroscopicity, which is defined through its effect on the water activity of the solution within the particle (Petters & Kreidenweis, 2007).

$$\kappa = \frac{V_w}{V_d} \frac{1 - a_w}{a_w} \quad (5)$$

V_w is the total ALWC volume in the aerosols (the sum of the volume based inorganic water content predicted by ISORROPIA2.1 and the estimated volume based organic water content), V_d is the total dry volume of species (the sum of volumes of the organic and inorganic species), and a_w is the water activity assumed to be equal to the RH values for the ambient condition. The dry volume of the inorganic mass was calculated by dividing the average inorganic mass concentration by an average value of inorganic density 1.6 g/cm³ (Lide, 2009) and the total volume of water contributed by inorganics was calculated by dividing the mass concentration of ALWC predicted from the model (considering only inorganics) by the density of water, 1 g/cm³.

The reverse mode calculation in ISORROPIA 2.1 is based on the assumption of a fixed chemical composition of the aerosol phase, irrespective of the RH. However, in the ambient, partitioning of chemical species between the gaseous and aerosol phases is enhanced with increase in RH, leading to aerosol growth and secondary aerosol formation (Gunthe et al., 2021; M. Saxena et al., 2017). Gas to particle partitioning would alter the chemical composition of the aerosol phase depending on the RH, and this indicates a strong dependence of particle phase chemical composition on RH. Gas to particle partitioning is modelled in the forward mode of ISORROPIA2.1, where the total species concentration consisting of both gaseous and aerosol phase is provided as input to the model and the species are partitioned between both the phases based on the RH and temperature. This calculation is not feasible in the present study due to lack of gas phase measurements and hence, the reverse mode is used. Since the particle phase chemical composition is assumed to be constant across all RH in reverse mode, κ , which is a function of chemical composition, could be calculated as a characteristic parameter for a given location. κ is thus estimated using Equation 5, by a fit between the V_w/V_d ratio and a_w , for a range of RH. The κ associated with the inorganics was also fitted separately, using only the inorganic dry mass and corresponding ALWC predicted by the model.

2.5 Estimation of ALWC combining WRF-Chem simulation with ISORROPIA2.1

Weather Research Forecasting (WRF) model coupled with Chemistry (WRF-Chem) was used to simulate the chemical composition of NH_4^+ , SO_4^{2-} , NO_3^- , and organics over the Indian region. Important details about the WRF-Chem version, domain, resolution, boundary conditions, meteorological and chemical fields, and emission inventory used for the WRF-Chem simulations are discussed elsewhere (Chutia et al., 2019). Briefly, the WRF-Chem simulations were carried out using the 3.9.1.1. version of the model with high spatial resolution of 12 km x 12 km for January 2011, using updated anthropogenic emission inventory Emissions Database for Global Atmospheric Research- Hemispheric Transport of Air Pollution (EDGAR - HTAP). The model output has been rigorously validated against the comprehensive gas phase observational data set of volatile organic compounds (VOC) over the Indian region for the month of January 2011. Model results over parts of India, particularly over the hot spots of anthropogenic emission, appeared to have reproduced the observational data with good qualitative and quantitative agreement (Chutia et al., 2019). We used the simulated NH_4^+ , SO_4^{2-} , NO_3^- , organic mass concentrations and RH over the Indian region (Figure S6), which was further coupled with ISORROPIA2.1 to derive the ALWC over the Indian region, with the same resolution

424 as that of the mass concentration of inorganic and organic compounds as that of WRF-
 425 Chem output.

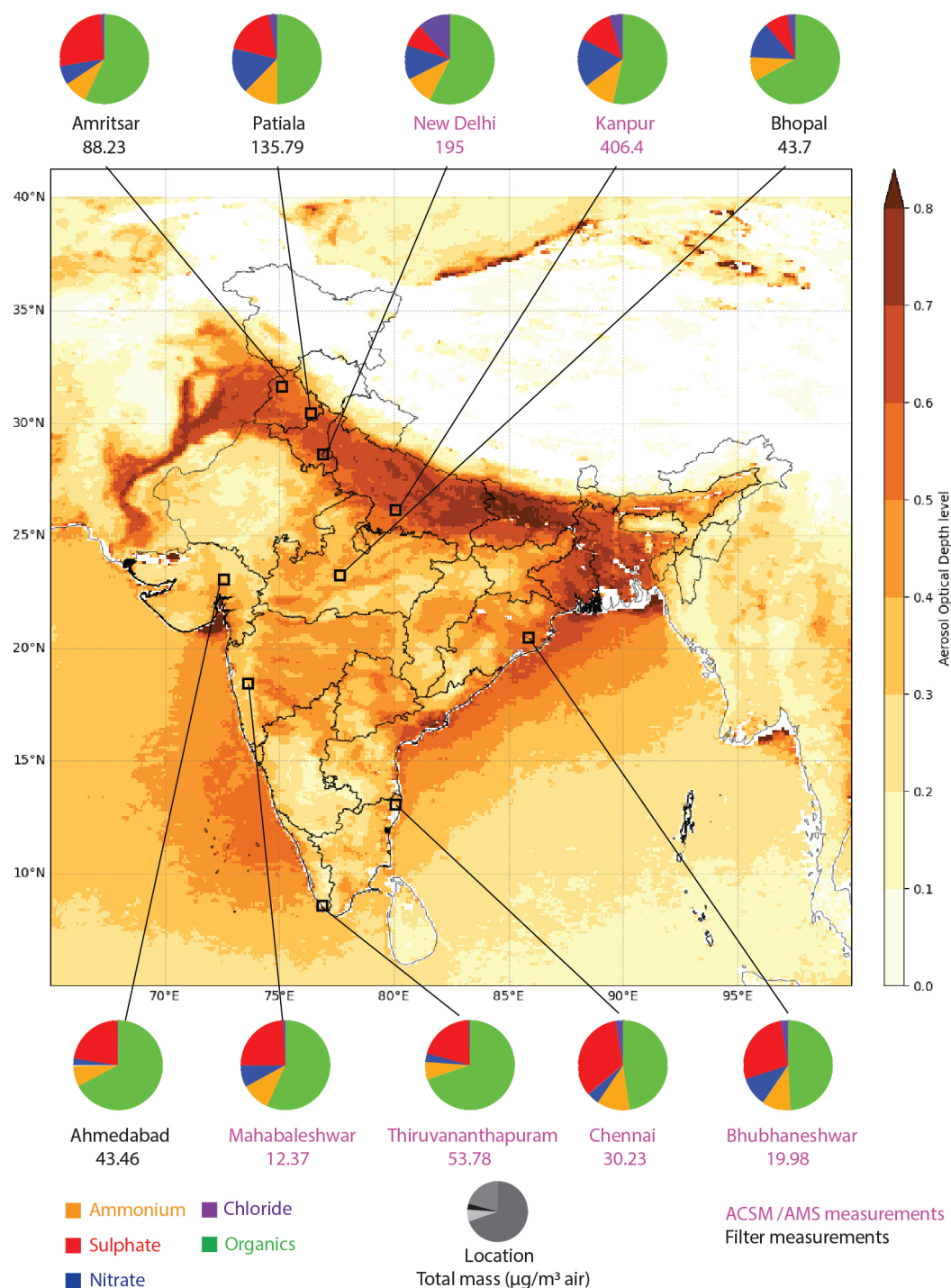


Figure 1. Average chemical composition of fine aerosols at locations over India during winter based on ACSM/AMS (violet text) or filter-based (black text) measurements. The pie charts represent the average fraction of different chemical species in the aerosols, at various measurement locations indicated by the solid lines and square markers on the map. The basemap depicts annual mean (year 2017) of AOD derived using Level 2 data from MODIS.

3 Results and discussion

3.1 Overview of ALWC over the Indian region

Figure 1 shows the spatial distribution of the annual mean of Aerosol Optical Depth (AOD) over the Indian region for the year 2017 using data from Moderate Resolution Imaging Spectroradiometer (MODIS), as a nominal representation of the spatial distribution of the aerosol loading over the Indian region. The Indo-Gangetic Plain (IGP), spread from the state of Punjab in the west to West Bengal in the east, is a hot spot of aerosol emissions, as evident from the figure. The AOD levels in the region are consistently greater than 0.5, with hotspots at some locations with AOD >0.8. The high aerosol loading in the IGP is attributed to dust transport, agricultural residue burning, solid biomass burning for domestic cooking and heating, persistent waste burning, and fossil fuel combustion from thermal power plants and vehicles (Ojha et al., 2020; Jat & Gurjar, 2021). Modelling studies have further reported the widespread enhancement of fine particulate matter across IGP especially during wintertime (Ojha et al., 2020). The average dry mass composition consisting of the measured secondary species (inorganic and organic) is marked in the figure as pie charts, using the data summarised in Table S2 for the corresponding locations on the map. The species composition was averaged over the measurement periods corresponding to the field studies carried out at respective locations, where the composition of PM_{1.0} was measured by online real-time Aerosol Mass Spectrometer (AMS)/ Aerosol Chemical Speciation Monitor (ACSM) (locations marked in violet text) and that of PM_{2.5} derived from filter based measurements (locations marked in black text). The pie charts evidently show chemical heterogeneity across the diverse environmental conditions for each locations under consideration. The total dry aerosol mass of PM_{1.0} and PM_{2.5}, determined as the sum of the mass concentrations of all measured species is also marked for the corresponding to the locations. For PM_{1.0}, the total dry aerosol mass ranged from the lowest value of 12.37 $\mu\text{g m}^{-3}$ at Mahabaleshwar- a pristine high-latitude location in the Western Ghats, to the highest value of 406.4 $\mu\text{g m}^{-3}$ at Kanpur- a hot spot of anthropogenic emissions in the IGP. The same for PM_{2.5} ranged from 43.46 $\mu\text{g m}^{-3}$ at Ahmedabad, to the highest value of 135.79 $\mu\text{g m}^{-3}$ at Patiala, which is also located in the IGP. The PM_{1.0} concentration in coastal locations is an order of magnitude lower than that at the continental locations, which may be due to dispersion of polluted air masses in the plain and favourable landscape, by air masses with higher wind speeds and of marine origin.

The observed chemical heterogeneity needs to be discussed in terms of the variation of the percentage of ionic species across diverse environmental conditions. The percentage of SO_4^{2-} in the dry mass ranges from 8.21% in New Delhi to 33.41% in Chennai in PM_{1.0}, and from 8.46% in Amritsar to 26.35% in Bhopal in PM_{2.5}. SO_4^{2-} is generally formed through different mechanisms of oxidation from the precursor SO_2 gas (A. Kumar & Sarin, 2010; Rengarajan et al., 2011; Deshmukh et al., 2016; Agarwal et al., 2020), which is predominantly emitted by combustion of coal used in thermal power plants (Rastogi et al., 2016; S. Kumar et al., 2018). The percentage of NO_3^- in the dry mass ranges from 3.14% in Thiruvananthapuram to 17.52% in Kanpur in PM_{1.0}, and from 2.76% in Ahmedabad to 16.45% in Patiala in PM_{2.5}. NO_3^- is formed through gas to particle conversion of precursor NO_x gases (Rengarajan et al., 2011; Deshmukh et al., 2016), prominently emitted by fossil fuel combustion by automobiles (Rengarajan et al., 2011; Deshmukh et al., 2016; Agarwal et al., 2020). The percentage of Cl^- in the dry mass ranges from 0.45% in Thiruvananthapuram to 11.8% in New Delhi in PM_{1.0}, and from 0.18% in Ahmedabad to 2.87% in Patiala in PM_{2.5}. Continental Cl^- is dominantly due to anthropogenic emissions from biomass burning, open waste burning (mainly of plastics like PVC), and brick kilns, either as primary emission as particulates or secondary emission in the form of HCl vapour. (Engling et al., 2009; S. Kumar et al., 2015; P. Kumar & Yadav, 2016; Cao et al., 2016; Gunthe et al., 2021). Though Cl^- is naturally released as sea salt formed by wave crashing in the oceans, sea salt Cl^- is not expected in the PM_{2.5}

data under consideration since the quantified Cl^- is of continental nature. Nor is it expected in the $\text{PM}_{1.0}$ data under consideration in which the quantified Cl^- is of non-refractory nature. The percentage of NH_4^+ in the dry mass ranges from 6.42% in Thiruvananthapuram to 11.9% in Chennai in $\text{PM}_{1.0}$, and from 7.36% in Ahmedabad to 12.19% in Patiala in $\text{PM}_{2.5}$. NH_4^+ is mainly formed through gas to particle conversion of NH_3 gas through its reaction with acid precursors like H_2SO_4 , HNO_3 and HCl to form NH_4^+ salts of SO_4^{2-} , NO_3^- and Cl^- (Finlayson-Pitts & Pitts, 2000; Singh & Kulshrestha, 2012; Deshmukh et al., 2016; S. K. Sharma et al., 2020). Thus, NH_3 is an important precursor for SO_4^{2-} , NO_3^- and Cl^- formation in $\text{PM}_{2.5}$ and hence acts as an important driver for the formation of secondary inorganic aerosols in the fine mode (M. Sharma et al., 2007). NH_3 is mainly emitted from decomposition of animal waste, fertilizer use (in the form of NH_3 or urea), conversion of NO_x to elemental nitrogen in catalytic converters installed in vehicles and biomass burning (M. Sharma et al., 2007; A. Kumar & Sarin, 2010; Aneja et al., 2012; Singh & Kulshrestha, 2012; Yadav & Kumar, 2014). Organic matter is observed to contribute a significant fraction of the total aerosol mass burden over all locations, ranging from 47.64% in Chennai to 69.73% in Thiruvananthapuram in $\text{PM}_{1.0}$, and from 50.17% in Patiala to 67.37% in Ahmedabad in $\text{PM}_{2.5}$ (estimated from OC measurements). Organic matter is emitted from biomass and fossil fuel burning prominently. Biomass burning accounts for 70% of the total carbonaceous aerosol emissions in India, as noted in emission inventory models (Örjan Gustafsson et al., 2009). Further photochemical oxidation reactions and condensation of organic vapors may lead to formation of WSOC (Faust et al., 2017). Organic matter contributes more than 50% of the total aerosol mass burden at almost all locations under consideration. Thus, it is expected to play an important role in determining the water uptake characteristics at various locations, subject to the assumption of limited hygroscopicity of organics ($\kappa=0.08$ or 0.13) (Nguyen et al., 2016).

Figure S1 shows the minimum, average and maximum RH at various Indian locations during wintertime. The dots represent the average RH while the whiskers represent the maximum and minimum RH for the corresponding locations. It is observed that the minimum, average, and maximum RH for the entire Indian region are on an average, around 35%, 70% and 95% respectively. Thus, ALWC was calculated for all the locations at these 3 values of RH using ISORROPIA2.1. An overview of the distribution of ALWC calculated at the average RH of 70% is given in Figure 2. The wet mass composition of aerosols, which includes the calculated ALWC is represented as pie charts, and they are labelled corresponding to the locations marked on the map. The fraction of ALWC in the aerosol wet mass is highlighted (coloured light blue) on the pie charts and its mass concentration (in $\mu\text{g m}^{-3}$ air) is also marked. The reported ALWC comprises of contributions by both organic and inorganic components of aerosols. The hygroscopicity parameter κ determined through fit, is displayed for every location (value enclosed within brackets) and the values have been summarised in Table S3. It is evident that ALWC is an important contributor to the total aerosol mass burden at all locations, irrespective of varying chemical composition, absolute PM mass and κ as evident from Figure 2. Thus, the ubiquity of ALWC in aerosols over the Indian region is reaffirmed. ALWC is observed to contribute around 25-35% of the total aerosol mass burden at the average RH of 70%. κ varies from 0.17 in Thiruvananthapuram to 0.28 at New Delhi and Kanpur in $\text{PM}_{1.0}$ dataset and 0.18 at Ahmedabad to 0.28 at Patiala in $\text{PM}_{2.5}$ data set.

3.2 Factors affecting ALWC over the Indian region

The variation of ALWC requires to be analysed with respect to the three factors governing it- RH, absolute dry mass concentration, and chemical composition. To further investigate the variation in the fraction of ALWC in the aerosol mass burden, the fractional wet aerosol composition at (a) 35%, (b) 70% and (c) 95% RH has been calculated and displayed in Figure 3. The fraction of total ALWC (which includes contribution by both organic and inorganic matter and coloured blue), is compared across the

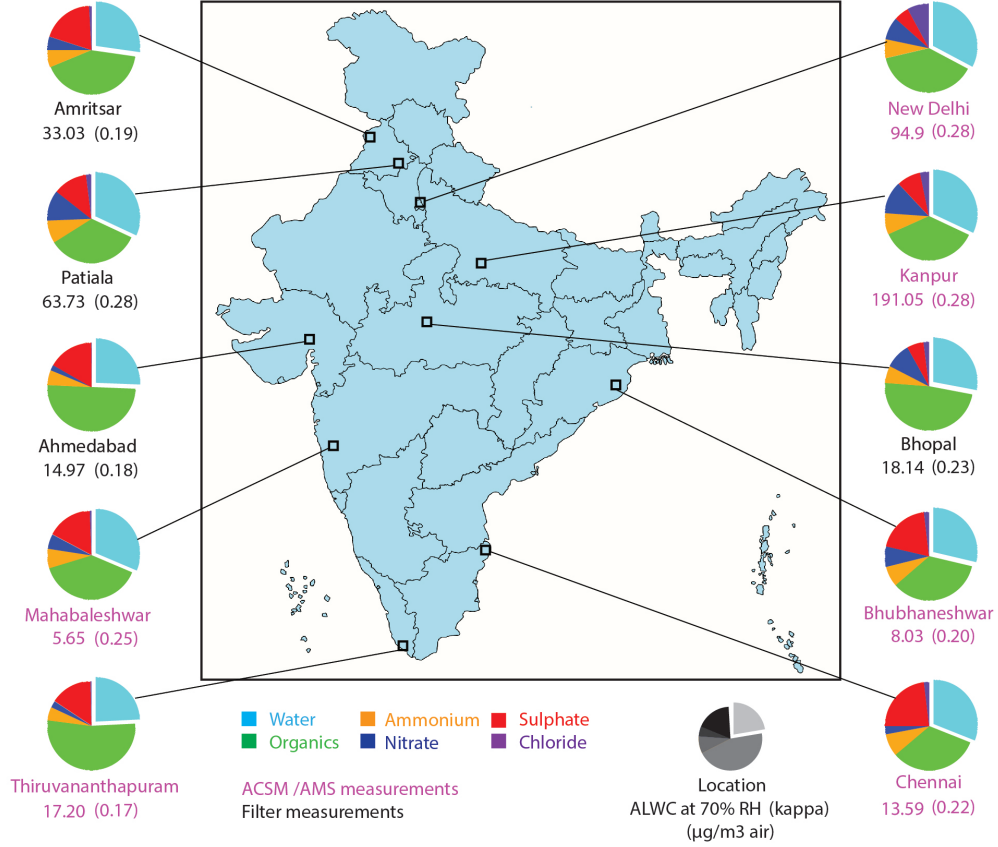


Figure 2. Fraction of ALWC modelled at the average RH of 70% during winter at various locations over India is shown as pie charts with the aerosol chemical composition. Solid lines and square markers denote the locations where measurements were done using either ACSM/AMS (violet text) or filter based methods (black text). The absolute mass of calculated ALWC ($\mu\text{g m}^{-3}$) and the hygroscopicity parameter kappa (in parenthesis) fitted for respective locations are marked beneath the respective pie charts.

diverse environmental conditions as shown in Fig. 3 for three different ambient RH levels separately. The percentage of ALWC is lowest at Thiruvananthapuram (8%, 24%, 68% corresponding to 35%, 70%, 95% RH) and highest at Chennai (13% corresponding to 35% RH), New Delhi (33%, 78% corresponding to 70%, 95% RH) in the $\text{PM}_{1.0}$ data set. For the $\text{PM}_{2.5}$ data set, the percentage of ALWC is lowest at Bhopal (8% corresponding to 35% RH), Ahmedabad (26%, 69% corresponding to 70%, 95% RH) and highest at Patiala (11%, 32%, 78% corresponding to 35%, 70%, 95% RH). The average percentage of ALWC is 11% for $\text{PM}_{1.0}$, 9% for $\text{PM}_{2.5}$ at 35% RH, 30% for $\text{PM}_{1.0}$, 28% for $\text{PM}_{2.5}$ at 70% RH and 74% for $\text{PM}_{1.0}$, 73% for $\text{PM}_{2.5}$ at 95% RH. The average percentage of ALWC is thus comparable for $\text{PM}_{1.0}$ and $\text{PM}_{2.5}$. The change in the ALWC percentage may be noted to be more pronounced from 70% to 95% RH compared to 35% to 70% RH. At 35% RH, the percentage of the total aerosol mass burden occupied by ALWC is minimal. Up to the average ambient RH level of 70% RH, the percentage of ALWC has increased steadily with RH, while a sharp increase occurs at 95% RH. At this RH, the ALWC appears to dominate the total aerosol mass burden significantly that at least 70% of the total mass is occupied by ALWC. Therefore, high RH drives ALWC to dominate the total mass, irrespective of the aerosol chemical composition. This observation is consistent with previous studies, which also observed that that under high RH con-

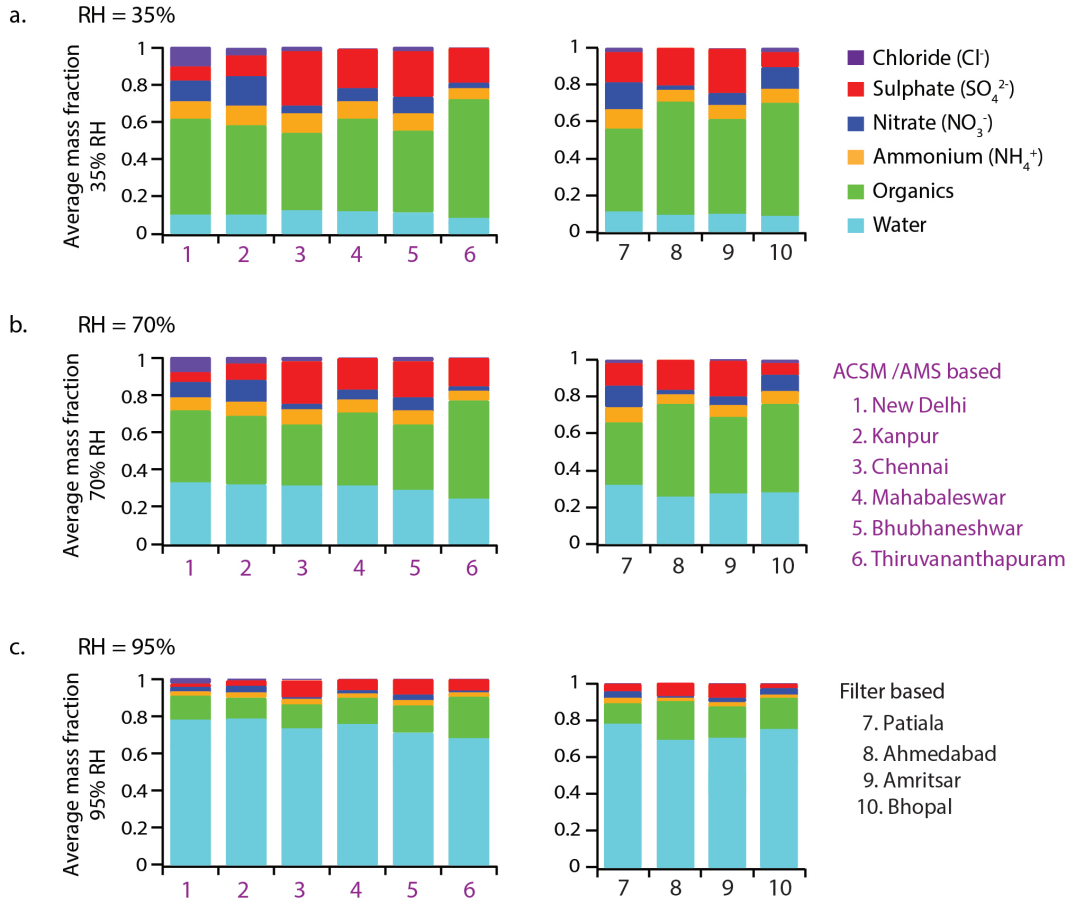


Figure 3. Comparison of the mass fraction of ALWC and chemical species in aerosols at relative humidity (a) 35%, (b) 70% and (c) 95%, (representing minimum, average and maximum RH during wintertime) between various locations over India indicated by the number on x-axis. ACSM/AMS based locations are indicated by violet text and filter based locations are indicated by black text.

ditions, ALWC is the highest contributor to the overall aerosol mass burden (Bian et al., 2014; Nguyen et al., 2016; Shen et al., 2019; Jin et al., 2020).

Though considerable uniformity has been observed in the fraction of ALWC in the total aerosol mass burden at a particular RH, the absolute ALWC is also strongly influenced by mass concentration and chemical composition. Figure 4 compares the water uptake characteristics between 35%, 70% and 95% RH at different locations. Figure 4a compares the calculated absolute ALWC at the three RH at every location. The total ALWC is highest at Kanpur (45.44, 191.05 and 1447.50 $\mu\text{g m}^{-3}$ air at 35%, 70% and 95% RH respectively) and lowest at Mahabaleswar (1.68, 5.65 and 37.84 $\mu\text{g m}^{-3}$ air at 35%, 70% and 95% RH respectively) among the $\text{PM}_{1.0}$ data set. Among the $\text{PM}_{2.5}$ data set, it is highest at Patiala (16.43, 63.73 and 470.81 $\mu\text{g m}^{-3}$ air at 35%, 70% and 95% RH respectively) and the lowest ALWC at Bhopal (4.28 $\mu\text{g m}^{-3}$ air at 35%) and Ahmedabad (14.97, 97.28 $\mu\text{g m}^{-3}$ air at 70% and 95% RH respectively). ALWC is thus observed to follow the same trend as that of the dry aerosol mass in terms of the locations, as discussed from Figure 1. Hence, the absolute value of ALWC is strongly dependent on the total mass concentration of aerosols. The ALWC contributed by inorganics is highest at Kanpur (38.76, 162.09 and 1211.68 $\mu\text{g m}^{-3}$ air at 35%, 70% and 95% RH respectively)

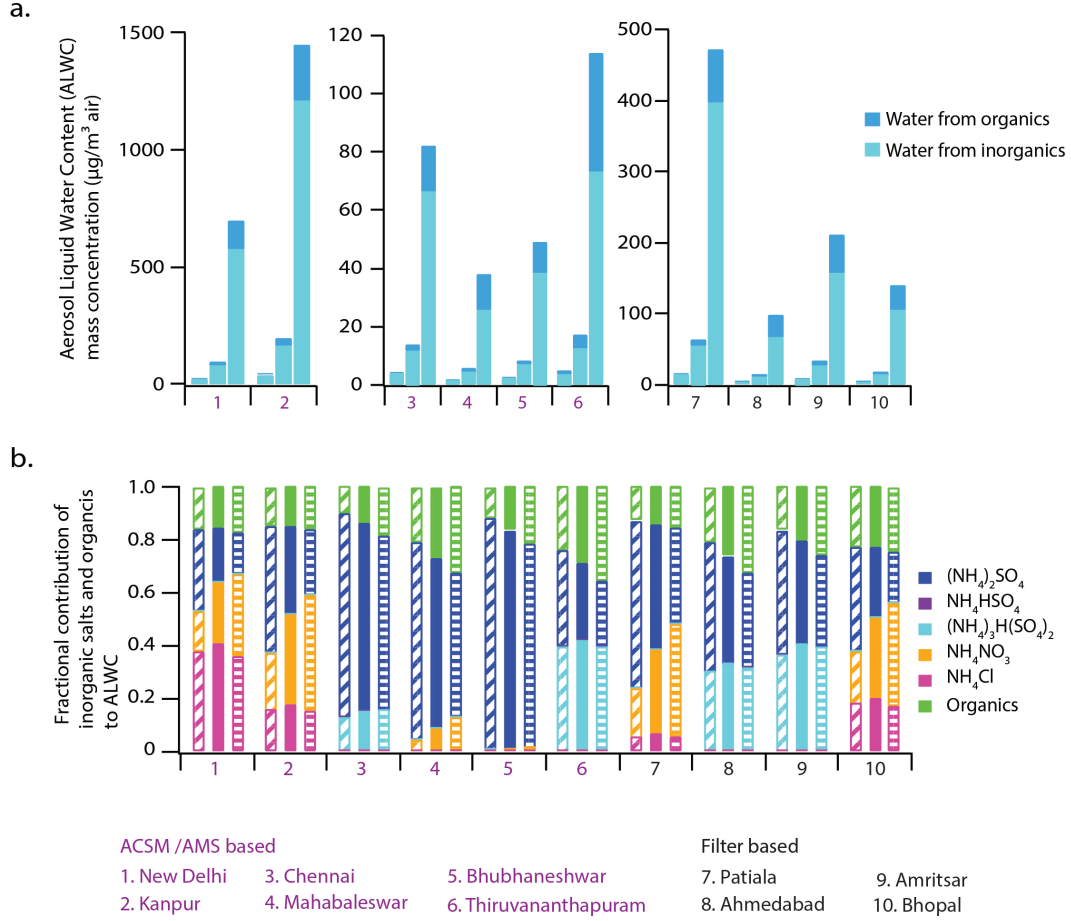


Figure 4. Comparison of water uptake characteristics at 35%, 70% and 95% RH (minimum, average and maximum RH during wintertime) are shown as respective bars for each selected location over India indicated by the number on x-axis. (a) ALWC contributed by organic and inorganic ($\mu\text{g m}^{-3}$ air) are marked in dark blue and light blue respectively on each bar (b) Fractional contribution to ALWC by inorganic salts and organic matter. ACSM/AMS based locations are indicated by violet text and filter based locations are indicated by black text.

and lowest at Mahabaleswar (1.33, 4.13 and $25.45 \mu\text{g m}^{-3}$ air at 35%, 70% and 95% RH respectively) among $\text{PM}_{1.0}$ data set. Among the $\text{PM}_{2.5}$ data set, it is highest at Patiala (14.33, 54.64 and $396.85 \mu\text{g m}^{-3}$ air at 35%, 70% and 95% RH respectively) and lowest at Bhopal ($3.25 \mu\text{g m}^{-3}$ air at 35%) and Ahmedabad (11.07 and $5.49 \mu\text{g m}^{-3}$ air at 70% and 95% RH respectively). The ALWC contributed by the organic matter is highest at Kanpur (6.68, 28.96 and $235.82 \mu\text{g m}^{-3}$ air at 35%, 70% and 95% RH respectively) and lowest at Bhubhaneshwar (0.3, 1.31 and $10.66 \mu\text{g m}^{-3}$ air at 35%, 70% and 95% RH respectively) among $\text{PM}_{1.0}$ data set. Among the $\text{PM}_{2.5}$ data set, it is highest at Patiala (2.1, 9.08 and $73.97 \mu\text{g m}^{-3}$ air at 35%, 70% and 95% RH respectively) and lowest at Ahmedabad (0.9, 3.9 and $31.79 \mu\text{g m}^{-3}$ air at 35%, 70% and 95% RH respectively).

These results show that a strong non-linear rise is observed in the ALWC, in either case of organic or inorganic contribution. ALWC is observed to rise slowly from 35% to 70% RH, and a sharp rise is observed from 70% to 95% RH, which resulted in a jump by an order of magnitude in absolute ALWC. Thus, the water uptake by aerosols is strongly dependent on ambient RH, recording a slower rise at lower RH, which shifts to a steeper

rise at higher RH. This observation is consistent with the non linear trend in the variation of water uptake per unit mass of individual inorganic species and organic matter with RH across the 35%-95% RH range, as shown in Figure S2a. The data for the water uptake per unit mass of inorganic salt species was obtained from ISORROPIA2.1 while that of organic matter was calculated separately using Equation 5 of the κ -Kohler theory, assuming an average value of $\kappa_{org}=0.1$. Hence, the observed non linearity in the variation of the total ALWC for a location with RH, may also be represented by Equation 5. The plot between the ratio of the volume of water V_w and the volume of dry mass V_d ratio with a_w (or RH) is observed to give a near perfect fit with a single parameter κ , with correlation of fit, $R^2 > 0.99$ in all cases. The results of the fit are summarised in Table S3. κ characterises the particle hygroscopicity, in Equation 5, which relates water uptake, dry aerosol mass and RH. κ has been determined for the total chemical composition (inorganic+organic matter), as well as just the inorganic matter separately to obtain κ_{total} and κ_{inorg} , respectively. κ_{org} has also been tabulated for all locations assuming limited hygroscopicity ($\kappa_{org} = 0.08$ or 0.13 for urban and rural locations respectively) as discussed in the methodology.

Figure S3 shows the variation of water uptake per unit dry mass with RH for κ ranging from 0.1 to 0.6 in increments of 0.05, using Equation 4 of the κ -Kohler theory. The water uptake per unit dry mass (M_w/M_d) corresponds to V_w/V_d in Equation 4 and the water activity corresponding to RH was varied from 0.35 to 0.95. The non linear trend described earlier is clearly evident from the figure, but the steepness of rise depends on the κ . It can be observed that at lower RH, M_w/M_d is comparable for all κ , while at higher RH, M_w/M_d varies drastically for different κ . Hence, high κ may not enhance ALWC significantly at low RH as observed in previous studies (Tan et al., 2017). At lower RH range, the absolute dry mass would primarily determine the absolute ALWC. The critical value of RH as discussed in Jin et al. (2020), beyond which non linear rise occurs may be observed to be dependent on κ . Equation 4 may also be expressed as-

$$ALWC = M_d \cdot \kappa \cdot f(RH) \quad (6)$$

Equation 6 shows that at a particular RH level, ALWC would depend on the dry mass concentration and particle hygroscopicity. In this study, we observe that the range of predicted κ is confined to a relatively narrow range of 0.17 to 0.28, which would be significant only at higher RH as observed from Figure S3. Hence, it may be assumed that absolute dry mass concentration plays a dominant role in determining ALWC compared to the particle hygroscopicity, which is more significant at higher RH. In the ambient, high ALWC at higher RH conditions serves as a reactor for gas to particle reactions, leading to favourable conditions of secondary aerosol formation and growth, provided there is sufficiently high concentration of gaseous precursors available in the atmosphere (Cheng et al., 2016; G. Wang et al., 2016; Huang et al., 2014; Z. Wu et al., 2018). This leads to enhanced mass of the aerosol phase with enhanced hygroscopicity due to uptake of secondary inorganic species, which further enhances ALWC. This indicates that in the ambient atmosphere, non linearity in the variation of ALWC with respect to RH would be even steeper, with a strong dependence of the particle hygroscopicity on RH. Due to lack of gaseous measurement data, we are restricted to the reverse mode of ISORROPIA2.1 for ALWC calculations, assuming fixed composition of the particle phase with respect to RH. Hence κ , a parameter for particle phase chemical composition, does not consequently vary with RH in this study, enabling us to parameterise a single value of κ for a particular location irrespective of RH. Though this assumption doesn't represent the ambient, it should be noted that the chemical composition data used for the analysis consists of chemical concentration data averaged over a considerable period of time, which would experience varying RH. Hence, the chemical composition data is expected to be reasonably averaged that it would give a reasonable estimate of κ for a location. The calculations, especially at higher RH may provide a reasonable lower bound estimate for

ALWC. κ predicted by this method also acts as a simple parameter for a location, facilitating the prediction of water uptake of aerosols for the location at any RH. The methodology followed here allows for a robust derivation of water uptake characteristics of aerosols using traditional measurements of aerosol chemical composition, which could be used to model aerosol hygroscopicity in aerosol chemistry, transport and climate models with simple formulation.

While ALWC has been observed to be highly dependent on RH, it is also interesting to observe how different chemical species contribute to ALWC at different RH. Figure 4b shows the fractional contribution of organic matter and inorganic salt species to the ALWC across the three RH under consideration. ISORROPIA2.1 was used to predict the combinations of ionic species that make up the salts. In the $\text{NH}_4^+ - \text{SO}_4^{2-} - \text{NO}_3^- - \text{Cl}^-$ system, ISORROPIA2.1 predicts 3 regimes of salt species based on the ratio of the molar concentrations of NH_4^+ and SO_4^{2-} , quantified as the sulphate ratio (R_{SO_4}). The regimes are briefly described in Table S4. From Figure 4b, the data set under analysis appears to fall under only two regimes (ii) and (iii). New Delhi, Kanpur, Mahabaleshwar, and Bhubhaneshwar among the $\text{PM}_{1.0}$ data set and Patiala and Amritsar among the $\text{PM}_{2.5}$ data set fall under the ammonium rich regime. In this regime, ISORROPIA2.1 neutralises NH_4^+ with the anions in the order- SO_4^{2-} , NO_3^- and then Cl^- . Aerosols at these locations are observed to be rich in NH_4^+ , that they could neutralise SO_4^{2-} completely as $(\text{NH}_4)_2\text{SO}_4$, and then the excess NH_4^+ could neutralise NO_3^- and Cl^- wherever present. The model has predicted NH_4NO_3 at all locations in this regime, implying the presence of excess and enough NH_4^+ for NO_3^- neutralisation. However, only at New Delhi and Kanpur in the $\text{PM}_{1.0}$ has the model predicted NH_4Cl formation. Chennai and Thiruvananthapuram among $\text{PM}_{1.0}$ data set, and Ahmedabad and Bhopal among the $\text{PM}_{2.5}$ data set fall under the sulphate rich regime, where NH_4^+ is insufficient to neutralise SO_4^{2-} - that $(\text{NH}_4)_2\text{SO}_4$, NH_4HSO_4 and the double salt of sulphate and bisulphate $(\text{NH}_4)_3\text{H}(\text{SO}_4)_2$ are expected to form. However, in the present analysis, NH_4HSO_4 out of the three salts have not been predicted at any of the locations. Across all locations in the Indian region and at all RH, the contribution of organic matter to ALWC is much lower than that by inorganic matter. The assumption of limited hygroscopicity for organic matter could also be the reasons for the low contribution to ALWC despite organics being the species with the highest mass fraction in the dry chemical composition. Data on WSOC concentration, which is available in the present data set, may be used for a better estimation of the water uptake, assuming higher hygroscopicity for secondary organics in future studies. Among the inorganic salt species, $(\text{NH}_4)_2\text{SO}_4$ remains the most prevalent contributor to ALWC across all locations in the Indian region. It is interesting to note that the fractional contribution of each species can be observed to vary with RH. The variation in the fractional contribution by organic matter and NH_4Cl with RH in regime (iii) locations does not show a stable trend. However, the fractional contribution of $(\text{NH}_4)_2\text{SO}_4$ clearly decreases with RH while that of NH_4NO_3 increases. This may be explained from Figure S2b where the water uptake by unit mass of individual species has been represented on a logarithmic scale for better visualisation. It is evident that $(\text{NH}_4)_2\text{SO}_4$ has higher water uptake than NH_4NO_3 at lower RH, which reverses after around 80% RH. A similar comparison between regime (ii) salts $(\text{NH}_4)_2\text{SO}_4$, NH_4HSO_4 and $(\text{NH}_4)_3\text{H}(\text{SO}_4)_2$ in Figure S2b shows that the water uptake by $(\text{NH}_4)_2\text{SO}_4 > \text{NH}_4\text{HSO}_4 > (\text{NH}_4)_3\text{H}(\text{SO}_4)_2$ at 35% RH and it changes to $\text{NH}_4\text{HSO}_4 > (\text{NH}_4)_3\text{H}(\text{SO}_4)_2 \approx (\text{NH}_4)_2\text{SO}_4$. These observations indicate the RH dependence of water uptake by individual salts. Further investigation of particle hygroscopicity is done in the subsequent section.

Since the present discussion focuses on ALWC corresponding to secondary inorganic species whose precursors are mainly from anthropogenic emissions, it is also necessary to observe the effect of K^+ ions released by bio mass burning activities on the ALWC. K^+ has been reported to be one of the dominantly emitted species during bio mass burning (Engling et al., 2009; Cao et al., 2016). Figure S4 compares the ALWC from inorganic species and the individual contribution by various inorganic species, in scenarios

where (i) K^+ ions were not considered in the analysis and (ii) K^+ ions were incorporated, at the average RH of 70%. Inorganic chemical composition data from three other locations- Mount Abu, Sikandarpur, and Patna, which satisfied the criteria of ammonium rich locations were also included in the comparison (the data could not be included in the main analysis due to lack of organic carbon measurements). Figure S4a compares the absolute inorganic ALWC in both the scenarios. The results indicate a negligible enhancement of ALWC with addition of K^+ at all locations. Figure S4b compares the contribution of inorganic salt species in both the scenarios. The only K^+ salt predicted is K_2SO_4 and it has a minimal contribution to the ALWC at all locations. However, the prediction of K_2SO_4 is questionable, since the major K^+ salt released from bio mass burning is reported to be KCl (Cao et al., 2016). KCl may undergo reactions with atmospheric H_2SO_4 and HNO_3 to form K_2SO_4 and KNO_3 respectively, the process being generally considered as the ageing of KCl evolved from bio mass burning emissions (Li et al., 2003). Moreover, ISORROPIA2.1 considers K^+ to be of crustal origin and also assumes internal mixing of all species (Fountoukis & Nenes, 2007). These observations suggest that K^+ of fresh bio mass burning may not be accurately modelled by the internally mixed assumption of ISORROPIA2.1. Since, the chemical composition data indicates low concentration of K^+ in the aerosols and the results show insignificant effect on the ALWC prediction, K^+ may be excluded from the analysis. Figure S2a shows the water uptake characteristics of the salts of K^+ . KCl is observed to have comparable hygroscopicity as NH_4Cl and K_2SO_4 and KNO_3 have very low hygroscopicity compared to other salt species. Since KCl is observed to have significant hygroscopicity, ALWC may be influenced by these species in regions of intense biomass burning, and the further analysis in this direction is beyond the scope of this study due to aforesaid reasons. We, however, intend to pursue this in followup studies.

3.3 Analysis of hygroscopicity

Figure 5 gives a comprehensive analysis of the hygroscopicity of aerosols under diverse environmental conditions considered in this study and the relative contribution of inorganic and organic matter. Figure 5a shows the line plot of the variation of the κ_{inorg} (marked pink) and κ_{total} (marked violet) across all the locations. As discussed earlier and as evident from Figure 2, the highest κ_{total} was observed to be 0.28 at New Delhi and Kanpur and the lowest to be 0.17 at Thiruvananthapuram among $PM_{1.0}$ based locations, while the highest κ_{total} for $PM_{2.5}$ based locations was observed to be 0.28 at Patiala and the lowest to be 0.18 at Ahmedabad. The highest κ_{inorg} was observed to be 0.59 at New Delhi and the lowest to be 0.33 at Bhubhaneshwar among $PM_{1.0}$ based locations. For $PM_{2.5}$ based locations, the highest κ_{inorg} was observed to be 0.58 at Bhopal and the lowest to be 0.36 at Amritsar.

As expected, κ_{total} is lower than the inorganic kappa at all locations due to the effect of the organic matter, which was assumed to have limited solubility in this study. The extent of lowering seemed to vary non uniformly and hence the contribution of organic matter to κ_{total} needs to be elucidated. Equation 5, may be redefined for multi-component mixtures using the κ mixing rule-

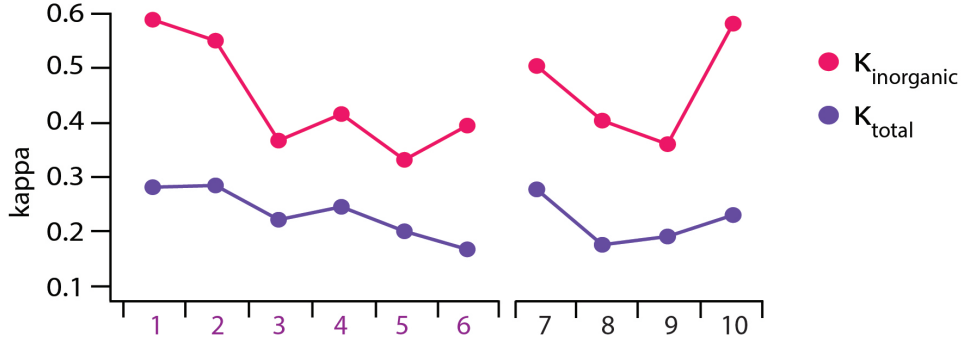
$$\kappa_{total} = \sum_i \kappa_i \epsilon_i \quad (7)$$

where κ_i and ϵ_i are the hygroscopicity parameter and volume fraction of the individual component i in the mixture. This mixing rule may be represented in terms of organic and inorganic fractions as-

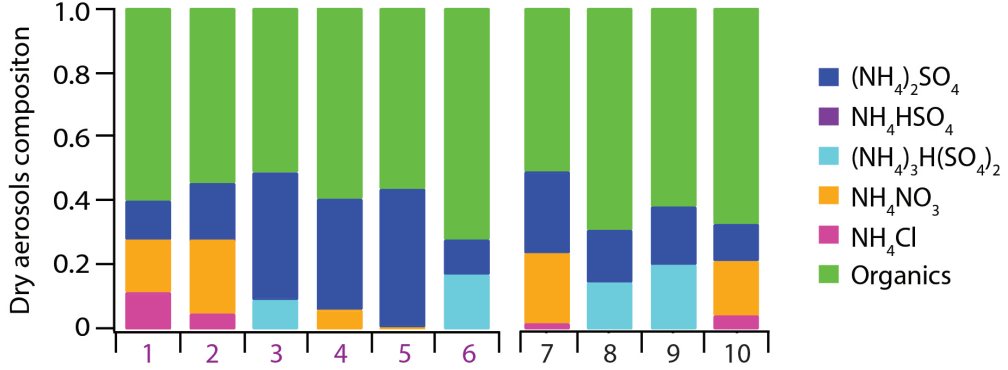
$$\kappa_{total} = \kappa_{inorg} \cdot (1 - f_{org}) + \kappa_{org} \cdot f_{org} \quad (8)$$

Equation 8 parameterises the hygroscopicity of inorganic and organic species (κ_{inorg} and κ_{org} respectively) separately and relates them to κ_{total} . f_{org} and f_{inorg} represent vol-

a.



b.



ACSM /AMS based

1. New Delhi 3. Chennai 5. Bhubhaneshwar
2. Kanpur 4. Mahabaleswar 6. Thiruvananthapuram

Filter based

7. Patiala 9. Amritsar
8. Ahmedabad 10. Bhopal

Figure 5. Comparison of hygroscopicity and chemical composition of aerosols across locations indicated by numbers on the x-axis. (a) Variation of inorganic hygroscopicity ($\kappa_{\text{inorganic}}$) and total hygroscopicity (κ_{total}) across locations (b) The fractional chemical composition of the dry aerosols, in terms of salt species. ACSM/AMS based locations are indicated by violet text and filter based locations are indicated by black text.

umetric fraction of organic and inorganic matter respectively. Considering that chemical compositions are generally expressed in terms of mass, it is more convenient to express the mixing rule in terms of mass fractions. Such a mixing rule had been earlier suggested by (Gunthe et al., 2009), where the assumption of mass fraction was made as a first order approximation. The relative error caused by the assumption of mass fraction was examined by comparing κ_{total} with κ_{mix} calculated using the mass fraction based mixing rule. Figure S5 shows that κ_{total} and κ_{mix} follow the 1:1 line with a correlation of fit of $R^2=0.85$ (considering only the 10 data points available). Hence, the assumption of mass fraction is not expected to cause significant error in the estimation of κ_{total} . The mixing rule was thus modified to the following form, representing the lowering of κ_{inorg} to κ_{total} as-

$$\kappa_{\text{inorg}} - \kappa_{\text{total}} = f_{\text{org}} \cdot (\kappa_{\text{inorg}} - \kappa_{\text{org}}) \quad (9)$$

Thus, the lowering of κ_{inorg} to κ_{total} due to the effect of organic matter, is a function of the fraction of organic matter f_{org} as well as the difference between κ_{inorg} and κ_{total} .

The organic fraction ranges between 50%-70% of the total aerosol mass and the relative difference between κ_{inorg} and κ_{org} changes considerably across locations too and hence, a combination of both factors determine the final κ_{total} . Figure 5b represents the dry chemical composition of the aerosols, where the inorganic species are in terms of the salt species. Observing κ_{inorg} from Figure 5a and the chemical composition in Figure 5b simultaneously, aerosols in regime (iii) are observed to have a slightly higher hygroscopicity compared to those in regime (ii). From Figure S2b, NH_4Cl appears to be the most hygroscopic salt among salts of NH_4^+ across the range. As earlier observed, NH_4NO_3 takes up more water compared to salts of NH_4^+ and SO_4^{2-} at higher RH, while at lower RH, the trend is reversed. Thus, NH_4Cl and NH_4NO_3 are responsible for the enhanced κ_{inorg} in regime (iii) relative to regime (ii). Earlier studies have reported higher κ for NH_4Cl and NH_4NO_3 (Petters & Kreidenweis, 2007; Jin et al., 2020; H. J. Liu et al., 2014), thus corroborating our observation. However, salts of NH_4^+ and SO_4^{2-} remain the most prevalent species in aerosols across the Indian region over the entire range of environmental conditions investigated here.

3.4 Spatial variation in ALWC

Figure 6 shows the ALWC over Indian region as calculated by ISORROPIA2.1 using the concentration of chemical species- NH_4^+ , SO_4^{2-} , NO_3^- and organic matter from WRF-Chem simulations. The spatial variation of the mass concentration of these chemical species over the Indian region is shown in Figure S6. Since Cl^- has been observed to be significant in ALWC calculations in the preceding section, lack of Cl^- concentration data from WRF-Chem may have implications on the predicted ALWC at some locations. Figure 6a shows the distribution of ALWC over the Indian region based on the spatial variation of relative humidity estimated for January 2011 by WRF-Chem simulations. West and east IGP appear to be the hotspot of ALWC, across a significant area. Scattered peaks in ALWC appear along the southern and eastern coastal areas, as well as the North east. Parts of West, Central and South West India display low ALWC concentration. Figure 6b, 6c, 6d represent the distribution of ALWC over the region, calculated at the three RH under consideration- 35%, 70% and 95%. The distribution of ALWC is similar across the three RH, with high ALWC in the IGP, south India and parts of the Western coast and low ALWC at Jammu and Kashmir and parts of North East India at the upper heights of the Himalayas. ALWC has been plotted for these plots on the same colour scale ranging between 0.1 to 700 $\mu\text{g m}^{-3}$ air.

In adherence to previous discussions, regarding the major factors affecting ALWC, the spatial variation plots of ALWC need to be discussed with reference to aerosol dry mass and RH. Figure S7 shows the spatial variation of (a) relative humidity and (b) the total aerosol dry mass calculated as the sum of the mass concentration of all species displayed in Figure S6. High relative humidity is observed in the IGP, eastern and southern coastal areas, Jammu and Kashmir and over North East India. The aerosol dry mass, however, peaks in West and East IGP compared to the rest of the Indian region. This observation coincides with the trend of absolute ALWC, and hence, it may be inferred that absolute aerosol dry mass is the primary driver of high ALWC, supported by conditions of high RH. The spatial variation of chemical species in Figure S6 suggests that west and east IGP are hotspots of NH_4^+ and NO_3^- . As discussed earlier, NH_3 is a driver for secondary particle formation from precursor acidic gases like SO_2 , NO_x and HCl . Thus, high NH_3 emissions in the IGP possibly lead to aggravated secondary particle formation under high RH (Figure S7a) conditions, which are particularly persistent during the winter season. The impact of secondary particle formation manifests as high PM loading (Figure S7b), which further results in the high ALWC observed in these regions (Figure 6).

Analysis of the spatial distribution of prospective salt species formed from the WRF based ionic species concentration has been performed using the dry mode of ISORROPIA2.1

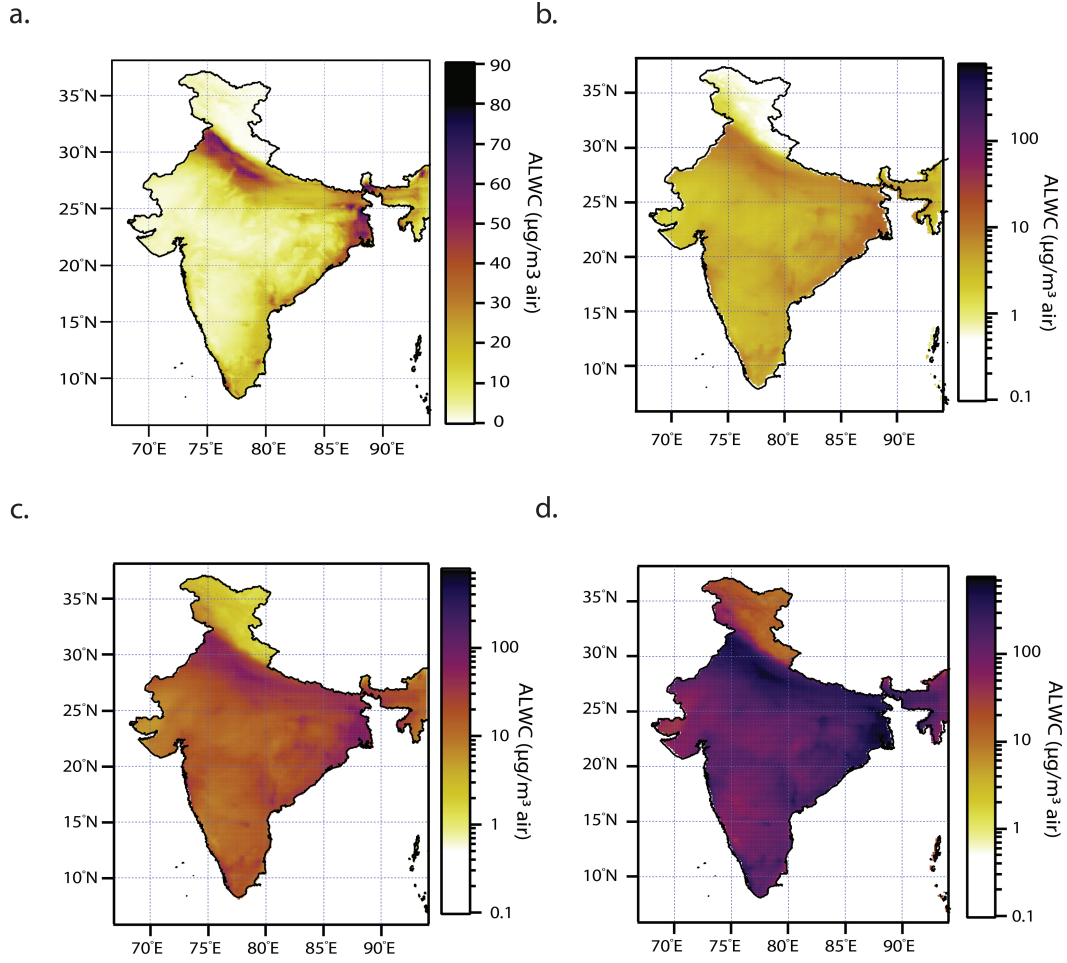


Figure 6. Spatial variation of ALWC (μgm^{-3} air) over India for January, modelled by ISOR-ROPIA2.1 using chemical concentration data of NH_4^+ , SO_4^{2-} , NO_3^- and organic matter from WRF CHEM model at (a) region specific RH modelled by WRF CHEM (b) fixed RH of 35%, (c) 70% and (d) 95% RH (representing the minimum, average and maximum RH respectively during winter).

(as discussed earlier) and the results are shown in Figure S8. The model predicts SO_4^{2-} to be high at higher concentrations over the Central- Eastern India, South India, and coastal Indian region (Figure S4), which is consistent with previous studies (Mallik et al., 2019). Hence, $(\text{NH}_4)_2\text{SO}_4$ is observed to be the dominant salt species over these regions as expected (Figure S8b), and may be responsible for the scattered peaks of ALWC observed in the region. The IGP is observed to be a hotspot of NH_4NO_3 (Figure S8a) as expected from the high concentration of NH_4^+ and NO_3^- in the region (Figure S7). NH_4NO_3 is stable only at low temperature and high RH (Adams et al., 1999; Deshmukh et al., 2016) and may be expected to be a dominant salt species in the aerosols as predicted.

The region experiences severe haze and smog during winter, which may hence be attributed to high PM loading over this region, with conditions further aggravated by high RH, which lead to enhancement of secondary aerosol formation and high ALWC. The observations in this study suggest that high NH_3 concentration in the region is a primary driver for the pollution load leading to harsh weather conditions. Furthermore, high NO_x emissions supplementing NH_3 provide a additional resource for the formation of the secondary inorganic aerosols, especially at high RH where NH_4NO_3 has been observed to have enhanced water uptake. This study also re-emphasises the importance of improvised pollution control strategies targeting emissions of specific chemical species- NH_3 and NO_x for improvement of ambient air quality in the Indian region.

4 Conclusions

A comprehensive analysis was performed to elucidate the role of aerosol mass concentration, composition and ambient relative humidity on the water uptake characteristics of fine mode aerosols (comprising SO_4^{2-} , NO_3^- , Cl^- , NH_4^+ and organic matter) over the Indian region during wintertime. ALWC was derived for $\text{PM}_{2.5}$ at six locations and $\text{PM}_{1.0}$ at four locations using the thermodynamic model ISOROPPIA2.1 at 35%, 70% and 95% RH, representing the minimum, average, and maximum RH during wintertime in the region. The presented analyses is strongly in line with previous literature indicating the ubiquitous nature of ALWC such that it constitutes a significant fraction of the total aerosol mass burden at the average ambient RH. It was observed that ALWC emerges as the most dominant component of atmospheric aerosols at very high RH, where its mass could be 2-3 times that of the dry aerosol mass. The absolute value of ALWC is strongly dependent on the absolute dry mass concentration, implying that high ALWC is primarily due to heavy pollution load, further enhanced by high ambient RH. Strong non-linear dependence of ALWC on RH is observed, which increases slowly at lower RH, and evolves to a sharp rise beyond the critical RH, as discussed in Jin et al. (2020). The critical RH was observed to depend on the particle hygroscopicity modelled as κ . The non-linear rise may be further enhanced at locations where secondary aerosol formation at conditions at high RH may result in enhanced particle hygroscopicity due to formation of hygroscopic secondary inorganic species. However, at low RH, ALWC was observed to be dependent on the absolute dry mass and not the particle hygroscopicity.

The key inorganic salt species predicted at the locations include $(\text{NH}_4)_2\text{SO}_4$, NH_4HSO_4 and $(\text{NH}_4)_3\text{H}(\text{SO}_4)_2$ at sulphate rich locations and $(\text{NH}_4)_2\text{SO}_4$, NH_4NO_3 and NH_4Cl at ammonium rich locations. NH_4NO_3 and NH_4Cl are formed at those locations with excess NH_4^+ after neutralising SO_4^{2-} , and are observed to raise the κ of aerosols substantially, compared to the salts of NH_4^+ and SO_4^{2-} . Organic matter, subject to the assumption of limited hygroscopicity, was observed to have a low contribution to the ALWC. High mass fraction of organic matter reduced the overall κ_{total} significantly at some locations. The spatial distribution of ALWC was calculated using the chemical composition of SO_4^{2-} , NO_3^- , NH_4^+ , organic matter and RH derived from WRF-Chem simulations. High PM loading, complemented by high RH was observed to drastically enhance the ALWC in the Indo-Gangetic Plain (IGP) region, which seems to explain the occurrence of haze and smog over the region. The distribution of ALWC across the Indian region at fixed RH revealed similar trends in variation at all three RH levels. Further, analysis of the occurrence of various salt species revealed that NH_4NO_3 is the primary cause of high ALWC over the IGP, while $(\text{NH}_4)_2\text{SO}_4$ dominated the peninsular region. The IGP region may benefit from the reduction of NH_4^+ and NO_3^- over SO_4^{2-} , due to observed higher hygroscopicity and abundance of NH_4NO_3 over other salts. The methods and assumptions used in this study may be utilised for a general analysis of the hygroscopic characteristics of aerosols for the given environmental conditions, using simple measurements of respective chemical composition. We further argue that analysis of ALWC under contrasting environments and covering distinct seasons is necessary alongside long-

term measurements of the aerosol chemical composition to better understand regional aerosol atmospheric chemistry and to mitigate extreme weather and climatic events related to ALWC.

Acknowledgement:

S.S.G. acknowledges partial funding from the Ministry of Earth Sciences (sanction number MoES/16/04/2017-APHH (PROMOTE)), the Government of India, and the Department of Science and Technology (sanction number DST/CCP/CoE/141/2018C), the Government of India. This work was partially supported by the UK Natural Environment Research Council with grant reference numbers NE/P016480/1 and NE/P016472/1. N.O. acknowledges the Vikram computing resources at the PRL, Ahmedabad. AKG acknowledges MHRD, Government of India for his M. Tech. fellowship. SSR was the recipient of a scholarship from the Indo-German Centre for Sustainability through the German Academic Exchange Service under the initiative “A New Passage to India” funded through the Federal Ministry for Education and Research in 2019 and 2020.

References

- Acharja, P., Ali, K., Ghude, S. D., Sinha, V., Sinha, B., Kulkarni, R., Gultepe, I., & Rajeevan, M. N. (2022). Enhanced secondary aerosol formation driven by excess ammonia during fog episodes in Delhi, India. *Chemosphere*, 289, 133155. doi: <https://doi.org/10.1016/j.chemosphere.2021.133155>
- Adams, P. J., Seinfeld, J. H., Koch, D., Mickley, L., & Jacob, D. (2001). General circulation model assessment of direct radiative forcing by the sulfate-nitrate-ammonium-water inorganic aerosol system. *Journal of Geophysical Research: Atmospheres*, 106(D1), 1097-1111. doi: <https://doi.org/10.1029/2000JD900512>
- Adams, P. J., Seinfeld, J. H., & Koch, D. M. (1999). Global concentrations of tropospheric sulfate, nitrate, and ammonium aerosol simulated in a general circulation model. *Journal of Geophysical Research: Atmospheres*, 104(D11), 13791-13823. doi: <https://doi.org/10.1029/1999JD900083>
- Agarwal, A., Satsangi, A., Lakhani, A., & Kumari, K. M. (2020). Seasonal and spatial variability of secondary inorganic aerosols in PM_{2.5} at Agra: Source apportionment through receptor models. *Chemosphere*, 242, 125132. doi: <https://doi.org/10.1016/j.chemosphere.2019.125132>
- Ajith, T., Kompalli, S. K., Nair, V. S., & Babu, S. S. (2022). Mesoscale variations of the chemical composition of submicron aerosols and its influence on the cloud condensation nuclei activation. *Atmospheric Environment*, 268, 118778. doi: <https://doi.org/10.1016/j.atmosenv.2021.118778>
- Alastuey, A., Querol, X., Castillo, S., Escudero, M., Avila, A., Cuevas, E., Torres, C., Romero, P.-M., Exposito, F., García, O., Diaz, J. P., Van Dingenen, R., & Putaud, J.-P. (2005). Characterisation of TSP and PM_{2.5} at Izana and Sta. Cruz de Tenerife (Canary Islands, Spain) during a Saharan Dust Episode (July 2002). *Atmospheric Environment*, 39, 4715-4728. doi: <https://doi.org/10.1016/j.atmosenv.2005.04.018>
- Almeida, G. P., Bittencourt, A. T., Evangelista, M. S., Vieira-Filho, M. S., & Fornaro, A. (2019). Characterization of aerosol chemical composition from urban pollution in Brazil and its possible impacts on the aerosol hygroscopicity and size distribution. *Atmospheric Environment*, 202, 149-159. doi: <https://doi.org/10.1016/j.atmosenv.2019.01.024>
- Aneja, V. P., Schlesinger, W. H., Erisman, J. W., Behera, S. N., Sharma, M., & Battye, W. (2012). Reactive nitrogen emissions from crop and livestock farming in India. *Atmospheric Environment*, 47, 92-103. doi: <https://doi.org/10.1016/j.atmosenv.2011.11.026>
- Arun, S. H., Sharma, S. K., Chaurasia, S., Vaishnav, R., & Kumar, R. (2018).

- Fog/low clouds detection over the Delhi Earth Station using the Ceilometer and the INSAT-3D/3DR satellite data. *International Journal of Remote Sensing*, 39(12), 4130-4144. doi: 10.1080/01431161.2018.1454624
- Babu, S. S., Manoj, M. R., Moorthy, K. K., Gogoi, M. M., Nair, V. S., Kompalli, S. K., Satheesh, S. K., Niranjana, K., Ramagopal, K., Bhuyan, P. K., & Singh, D. (2013). Trends in aerosol optical depth over Indian region: Potential causes and impact indicators. *Journal of Geophysical Research: Atmospheres*, 118(20), 11,794-11,806. doi: <https://doi.org/10.1002/2013JD020507>
- Balakrishnan, K., Dey, S., Gupta, T., Dhaliwal, R., Brauer, M., Cohen, A., Stanaway, J., Beig, G., Joshi, T., Aggarwal, A., Sabde, Y., Sadhu, H., Frostad, J., Causey, K., Godwin, W., Shukla, D., Kumar, G. A., Varghese, C., Muralidharan, P., & Dandona, L. (2018). The impact of air pollution on deaths, disease burden, and life expectancy across the states of India: the Global Burden of Disease Study 2017. *The Lancet Planetary Health*, 3. doi: 10.1016/S2542-5196(18)30261-4
- Bassett, M., & Seinfeld, J. H. (1983). Atmospheric equilibrium model of sulfate and nitrate aerosols. *Atmospheric Environment (1967)*, 17(11), 2237-2252. doi: [https://doi.org/10.1016/0004-6981\(83\)90221-4](https://doi.org/10.1016/0004-6981(83)90221-4)
- Bian, Y. X., Zhao, C. S., Ma, N., Chen, J., & Xu, W. Y. (2014). A study of aerosol liquid water content based on hygroscopicity measurements at high relative humidity in the North China Plain. *Atmospheric Chemistry and Physics*, 14(12), 6417-6426. doi: 10.5194/acp-14-6417-2014
- Boreddy, S. K. R., Hegde, P., & Aswini, A. R. (2021). Chemical Characteristics, Size Distributions, and Aerosol Liquid Water in Size-Resolved Coastal Urban Aerosols Allied with Distinct Air Masses over Tropical Peninsular India. *ACS Earth and Space Chemistry*, 5(3), 457-473. doi: 10.1021/acsearthspacechem.0c00282
- Canagaratna, M., Jayne, J., Jimenez, J., Allan, J., Alfarra, M., Zhang, Q., Onasch, T., Drewnick, F., Coe, H., Middlebrook, A., Delia, A., Williams, L., Trimborn, A., Northway, M., DeCarlo, P., Kolb, C., Davidovits, P., & Worsnop, D. (2007). Chemical and microphysical characterization of ambient aerosols with the aerodyne aerosol mass spectrometer. *Mass Spectrometry Reviews*, 26(2), 185-222. doi: <https://doi.org/10.1002/mas.20115>
- Cao, F., Zhang, S.-C., Kawamura, K., & Zhang, Y.-L. (2016). Inorganic markers, carbonaceous components and stable carbon isotope from biomass burning aerosols in Northeast China. *Science of The Total Environment*, 572, 1244-1251. doi: <https://doi.org/10.1016/j.scitotenv.2015.09.099>
- Chen, J., Zhao, C. S., Ma, N., Liu, P. F., Göbel, T., Hallbauer, E., Deng, Z. Z., Ran, L., Xu, W. Y., Liang, Z., Liu, H. J., Yan, P., Zhou, X. J., & Wiedensohler, A. (2012). A parameterization of low visibilities for hazy days in the North China Plain. *Atmospheric Chemistry and Physics*, 12(11), 4935-4950. doi: 10.5194/acp-12-4935-2012
- Cheng, Y., Zheng, G., Wei, C., Mu, Q., Zheng, B., Wang, Z., Gao, M., Zhang, Q., He, K., Carmichael, G., Pöschl, U., & Su, H. (2016). Reactive nitrogen chemistry in aerosol water as a source of sulfate during haze events in China. *Science Advances*, 2. doi: 10.1126/sciadv.1601530
- Chutia, L., Ojha, N., Girach, I. A., Sahu, L. K., Alvarado, L. M., Burrows, J. P., Pathak, B., & Bhuyan, P. K. (2019). Distribution of volatile organic compounds over Indian subcontinent during winter: WRF-chem simulation versus observations. *Environmental Pollution*, 252, 256-269. doi: <https://doi.org/10.1016/j.envpol.2019.05.097>
- Conibear, L., Butt, E. W., Knote, C., Arnold, S. R., & Spracklen, D. V. (2018). Residential energy use emissions dominate health impacts from exposure to ambient particulate matter in India. *Nature Communications*, 9(1), 617. doi: 10.1038/s41467-018-02986-7

- Cruz, C. N., & Pandis, S. N. (2000). Deliquescence and Hygroscopic Growth of Mixed Inorganic/Organic Atmospheric Aerosol. *Environmental Science & Technology*, 34(20), 4313-4319. doi: 10.1021/es9907109
- Dall'Osto, M., Harrison, R. M., Coe, H., & Williams, P. (2009). Real-time secondary aerosol formation during a fog event in London. *Atmospheric Chemistry and Physics*, 9(7), 2459-2469. doi: 10.5194/acp-9-2459-2009
- David, L. M., Ravishankara, A. R., Kodros, J. K., Pierce, J. R., Venkataraman, C., & Sadavarte, P. (2019). Premature Mortality Due to PM_{2.5} Over India: Effect of Atmospheric Transport and Anthropogenic Emissions. *GeoHealth*, 3(1), 2-10. doi: <https://doi.org/10.1029/2018GH000169>
- Deshmukh, D. K., Kawamura, K., & Deb, M. K. (2016). Dicarboxylic acids, ω -oxocarboxylic acids α -dicarbonyls, WSOC, OC, EC, and inorganic ions in wintertime size-segregated aerosols from central India: Sources and formation processes. *Chemosphere*, 161, 27-42. doi: <https://doi.org/10.1016/j.chemosphere.2016.06.107>
- Dougle, P., Vlasenko, A., Veefkind, J., & Ten Brink, H. (1996). Humidity dependence of the light scattering by mixtures of ammonium nitrate, ammonium sulfate and soot. *Journal of Aerosol Science*, 27, S513-S514. doi: [https://doi.org/10.1016/0021-8502\(96\)00329-1](https://doi.org/10.1016/0021-8502(96)00329-1)
- Engelhart, G. J., Moore, R. H., Nenes, A., & Pandis, S. N. (2011). Cloud condensation nuclei activity of isoprene secondary organic aerosol. *Journal of Geophysical Research: Atmospheres*, 116(D2). doi: <https://doi.org/10.1029/2010JD014706>
- Engling, G., Lee, J. J., Tsai, Y.-W., Lung, S.-C. C., Chou, C. C.-K., & Chan, C.-Y. (2009). Size-Resolved Anhydrosugar Composition in Smoke Aerosol from Controlled Field Burning of Rice Straw. *Aerosol Science and Technology*, 43(7), 662-672. doi: 10.1080/02786820902825113
- Fajardo, O. A., Jiang, J., & Hao, J. (2016). Continuous Measurement of Ambient Aerosol Liquid Water Content in Beijing. *Aerosol and Air Quality Research*, 16(5), 1152-1164. doi: 10.4209/aaqr.2015.10.0579
- Faust, J. A., Wong, J. P. S., Lee, A. K. Y., & Abbatt, J. P. D. (2017). Role of Aerosol Liquid Water in Secondary Organic Aerosol Formation from Volatile Organic Compounds. *Environmental Science & Technology*, 51(3), 1405-1413. (PMID: 28124902) doi: 10.1021/acs.est.6b04700
- Finlayson-Pitts, B., & Pitts, J. (2000). *chemistry of upper and lower atmosphere*.
- Fountoukis, C., & Nenes, A. (2007). ISORROPIA II: a computationally efficient thermodynamic equilibrium model for K^+ - Ca^{2+} - Mg^{2+} - NH_4^+ - Na^+ - SO_4^{2-} - NO_3^- - Cl^- - H_2O aerosols. *Atmospheric Chemistry Physics Discussions*, 7, 1893-1939. doi: 10.5194/acpd-7-1893-2007
- Gani, S., Bhandari, S., Seraj, S., Wang, D. S., Patel, K., Soni, P., Arub, Z., Habib, G., Hildebrandt Ruiz, L., & Apte, J. S. (2019). Submicron aerosol composition in the world's most polluted megacity: the Delhi Aerosol Super-site study. *Atmospheric Chemistry and Physics*, 19(10), 6843-6859. doi: 10.5194/acp-19-6843-2019
- Ghosh, A., Patel, A., Rastogi, N., Sharma, S. K., Mandal, T. K., & Chatterjee, A. (2021). Size-segregated aerosols over a high altitude Himalayan and a tropical urban metropolis in Eastern India: Chemical characterization, light absorption, role of meteorology and long range transport. *Atmospheric Environment*, 254, 118398.
- Ghosh, D., & Parida, P. (2015). Air Pollution and India: Current Scenario. *International Journal of Current Research*, 7, 22194-22196.
- Gunthe, S. S., King, S. M., Rose, D., Chen, Q., Roldin, P., Farmer, D. K., Jimenez, J. L., Artaxo, P., Andreae, M. O., Martin, S. T., & Pöschl, U. (2009). Cloud condensation nuclei in pristine tropical rainforest air of Amazonia: size-resolved measurements and modeling of atmospheric aerosol composition

- and CCN activity. *Atmospheric Chemistry and Physics*, 9(19), 7551–7575. doi: 10.5194/acp-9-7551-2009
- Gunthe, S. S., Liu, P., Panda, U., Raj, S. S., Sharma, A., Darbyshire, E., Reyes-Villegas, E., Allan, J., Chen, Y., Wang, X., et al. (2021). Enhanced aerosol particle growth sustained by high continental chlorine emission in India. *Nature Geoscience*, 14(2), 77–84.
- Guttikunda, S. K., & Goel, R. (2013). Health impacts of particulate pollution in a megacity—Delhi, India. *Environmental Development*, 6, 8–20. doi: <https://doi.org/10.1016/j.envdev.2012.12.002>
- Gysel, M., Crosier, J., Topping, D. O., Whitehead, J. D., Bower, K. N., Cubison, M. J., Williams, P. I., Flynn, M. J., McFiggans, G. B., & Coe, H. (2007). Closure study between chemical composition and hygroscopic growth of aerosol particles during TORCH2. *Atmospheric Chemistry and Physics*, 7(24), 6131–6144. doi: 10.5194/acp-7-6131-2007
- Hennigan, C. J., Bergin, M. H., Dibb, J. E., & Weber, R. J. (2008). Enhanced secondary organic aerosol formation due to water uptake by fine particles. *Geophysical Research Letters*, 35(18). doi: <https://doi.org/10.1029/2008GL035046>
- Huang, R.-J., Zhang, Y., Bozzetti, C., Ho, K.-F., Cao, J.-J., Han, Y., Daellenbach, K. R., Slowik, J. G., Platt, S. M., Canonaco, F., Zotter, P., Wolf, R., Pieber, S. M., Bruns, E. A., Crippa, M., Ciarelli, G., Piazzalunga, A., Schwikowski, M., Abbaszade, G., Schnelle-Kreis, J., Zimmermann, R., An, Z., Szidat, S., Baltensperger, U., Haddad, I. E., & Prévôt, A. S. H. (2014). High secondary aerosol contribution to particulate pollution during haze events in China. *Nature*, 514(7521), 218–222. doi: 10.1038/nature13774
- Jacobson, M. Z., Tabazadeh, A., & Turco, R. P. (1996). Simulating equilibrium within aerosols and non-equilibrium between gases and aerosols. *Journal of Geophysical Research: Atmospheres*, 101(D4), 9079–9091. doi: <https://doi.org/10.1029/96JD00348>
- Jain, S., Sharma, S. K., Srivastava, M. K., Chatterjee, A., Vijayan, N., Tripathy, S. S., Kumari, K. M., Mandal, T. K., & Sharma, C. (2021). Chemical characterization, source apportionment and transport pathways of PM_{2.5} and PM₁₀ over Indo Gangetic Plain of India. *Urban Climate*, 36, 100805. doi: <https://doi.org/10.1016/j.uclim.2021.100805>
- Jat, R., & Gurjar, B. R. (2021). Contribution of different source sectors and source regions of Indo-Gangetic Plain in India to PM_{2.5} pollution and its short-term health impacts during peak polluted winter. *Atmospheric Pollution Research*, 12(4), 89–100. doi: <https://doi.org/10.1016/j.apr.2021.02.016>
- Jin, X., Wang, Y., Li, Z., Zhang, F., Xu, W., Sun, Y., Fan, X., Chen, G., Wu, H., Ren, J., Wang, Q., & Cribb, M. (2020). Significant contribution of organics to aerosol liquid water content in winter in Beijing, China. *Atmospheric Chemistry and Physics*, 20(2), 901–914. doi: 10.5194/acp-20-901-2020
- Kaushik, A., Kumar, A., Anirudhan, A., Panda, P., Shukla, G., & Gupta, N. (2021). Seasonal Variation in Chemical Composition of Size-Segregated Aerosols Over the Northeastern Arabian Sea. *Frontiers in Environmental Science*, 8. doi: 10.3389/fenvs.2020.619174
- Kim, Y. P., Seinfeld, J. H., & Saxena, P. (1993). Atmospheric Gas-Aerosol Equilibrium I. Thermodynamic Model. *Aerosol Science and Technology*, 19(2), 157–181. doi: 10.1080/02786829308959628
- Kommula, S. M., Upasana, P., Sharma, A., Raj, S. S., Reyes-villegas, E., Liu, T., Allan, J. D., Jose, C., Pöhlker, M. L., Ravikrishna, R., Liu, P., Su, H., Martin, S. T., Pöschl, U., McFiggans, G., Coe, H., & Gunthe, S. S. (2021). Chemical Characterization and Source Apportionment of Organic Aerosols in the Coastal City of Chennai, India: Impact of Marine Air Masses on Aerosol Chemical Composition and Potential for Secondary Organic Aerosol

- Formation. *ACS Earth and Space Chemistry*, 5(11), 3197-3209. doi: 10.1021/acsearthspacechem.1c00276
- Kompalli, S. K., Suresh Babu, S. N., Satheesh, S. K., Krishna Moorthy, K., Das, T., Boopathy, R., Liu, D., Darbyshire, E., Allan, J. D., Brooks, J., Flynn, M. J., & Coe, H. (2020). Seasonal contrast in size distributions and mixing state of black carbon and its association with PM_{1.0} chemical composition from the eastern coast of India. *Atmospheric Chemistry and Physics*, 20(6), 3965–3985. doi: 10.5194/acp-20-3965-2020
- Krishna Moorthy, K., Suresh Babu, S., Manoj, M. R., & Satheesh, S. K. (2013). Buildup of aerosols over the Indian Region. *Geophysical Research Letters*, 40(5), 1011-1014. doi: <https://doi.org/10.1002/grl.50165>
- Kuang, Y., Zhao, C. S., Zhao, G., Tao, J. C., Xu, W., Ma, N., & Bian, Y. X. (2018). A novel method for calculating ambient aerosol liquid water content based on measurements of a humidified nephelometer system. *Atmospheric Measurement Techniques*, 11(5), 2967-2982. doi: 10.5194/amt-11-2967-2018
- Kulkarni, R., Jenamani, R., Pithani, P., Konwar, M., Nigam, N., & Ghude, S. (2019). Loss to Aviation Economy Due to Winter Fog in New Delhi during the Winter of 2011–2016. *Atmosphere*, 10, 198. doi: 10.3390/atmos10040198
- Kumar, A., & Sarin, M. (2010). Atmospheric water-soluble constituents in fine and coarse mode aerosols from high-altitude site in western India: Long-range transport and seasonal variability. *Atmospheric Environment*, 44(10), 1245-1254. doi: <https://doi.org/10.1016/j.atmosenv.2009.12.035>
- Kumar, A., Yadav, I., Shukla, A., & Devi, N. (2020). Seasonal Variation of PM_{2.5} in the Central Indo-Gangetic Plain (Patna) of India: Chemical Characterization and Source Assessment. *Journal of Applied Sciences*. doi: 10.1007/s42452-020-3160-y
- Kumar, P., & Yadav, S. (2016). Seasonal Variations in Water Soluble Inorganic Ions, OC and EC in PM₁₀ and PM_{>10} Aerosols over Delhi: Influence of Sources and Meteorological Factors. *Aerosol and Air Quality Research*, 16(5), 1165–1178. doi: 10.4209/aaqr.2015.07.0472
- Kumar, S., Aggarwal, S. G., Gupta, P. K., & Kawamura, K. (2015). Investigation of the tracers for plastic-enriched waste burning aerosols. *Atmospheric Environment*, 108, 49-58. doi: <https://doi.org/10.1016/j.atmosenv.2015.02.066>
- Kumar, S., Nath, S., Bhatti, M., & Yadav, S. (2018). Chemical Characteristics of Fine and Coarse Particles during Winter Time over Two Urban Cities in North India. *Aerosol and Air Quality Research*, 18. doi: 10.4209/aaqr.2018.02.0051
- Kumar, S., & Raman, R. (2016, 08). Inorganic ions in ambient fine particles over a National Park in central India: Seasonality, dependencies between SO₄²⁻, NO₃, and NH₄⁺, and neutralization of aerosol acidity. *Atmospheric Environment*, 143. doi: 10.1016/j.atmosenv.2016.08.037
- Kumari, S., Verma, N., Lakhani, A., & Kumari, K. M. (2021). Severe haze events in the Indo-Gangetic Plain during post-monsoon: Synergetic effect of synoptic meteorology and crop residue burning emission. *Science of The Total Environment*, 768, 145479. doi: <https://doi.org/10.1016/j.scitotenv.2021.145479>
- Lambe, A. T., Onasch, T. B., Massoli, P., Croasdale, D. R., Wright, J. P., Ahern, A. T., Williams, L. R., Worsnop, D. R., Brune, W. H., & Davidovits, P. (2011). Laboratory studies of the chemical composition and cloud condensation nuclei (CCN) activity of secondary organic aerosol (SOA) and oxidized primary organic aerosol (OPOA). *Atmospheric Chemistry and Physics*, 11(17), 8913–8928. doi: 10.5194/acp-11-8913-2011
- Lelieveld, J., Evans, J. S., Fnais, M., Giannadaki, D., & Pozzer, A. (2015). The contribution of outdoor air pollution sources to premature mortality on a global scale. *Nature*, 525(7569), 367-371. doi: 10.1038/nature15371
- Li, J., Pósfai, M., Hobbs, P. V., & Buseck, P. R. (2003). Individual aerosol particles from biomass burning in southern Africa: 2, Compositions and aging of inor-

- ganic particles. *Journal of Geophysical Research: Atmospheres*, 108(D13). doi: <https://doi.org/10.1029/2002JD002310>
- Liao, H., & Seinfeld, J. H. (2005). Global impacts of gas-phase chemistry-aerosol interactions on direct radiative forcing by anthropogenic aerosols and ozone. *Journal of Geophysical Research: Atmospheres*, 110(D18). doi: <https://doi.org/10.1029/2005JD005907>
- Lide, D. (2009). *CRC Handbook of Chemistry and Physics*. Taylor & Francis.
- Lin, Z. J., Tao, J., Chai, F. H., Fan, S. J., Yue, J. H., Zhu, L. H., Ho, K. F., & Zhang, R. J. (2013). Impact of relative humidity and particles number size distribution on aerosol light extinction in the urban area of Guangzhou. *Atmospheric Chemistry and Physics*, 13(3), 1115–1128. doi: 10.5194/acp-13-1115-2013
- Lin, Z. J., Zhang, Z. S., Zhang, L., Tao, J., Zhang, R. J., Cao, J. J., Fan, S. J., & Zhang, Y. H. (2014). An alternative method for estimating hygroscopic growth factor of aerosol light-scattering coefficient: a case study in an urban area of Guangzhou, South China. *Atmospheric Chemistry and Physics*, 14(14), 7631–7644. doi: 10.5194/acp-14-7631-2014
- Liu, H. J., Zhao, C. S., Nekat, B., Ma, N., Wiedensohler, A., van Pinxteren, D., Spindler, G., Müller, K., & Herrmann, H. (2014). Aerosol hygroscopicity derived from size-segregated chemical composition and its parameterization in the North China Plain. *Atmospheric Chemistry and Physics*, 14(5), 2525–2539. doi: 10.5194/acp-14-2525-2014
- Liu, P. F., Zhao, C. S., Göbel, T., Hallbauer, E., Nowak, A., Ran, L., Xu, W. Y., Deng, Z. Z., Ma, N., Mildenberger, K., Henning, S., Stratmann, F., & Wiedensohler, A. (2011). Hygroscopic properties of aerosol particles at high relative humidity and their diurnal variations in the North China Plain. *Atmospheric Chemistry and Physics*, 11(7), 3479–3494. doi: 10.5194/acp-11-3479-2011
- Mallik, C., Mahapatra, P. S., Kumar, P., Panda, S., Boopathy, R., Das, T., & Lal, S. (2019). Influence of regional emissions on SO₂ concentrations over Bhubaneswar, a capital city in eastern India downwind of the Indian SO₂ hotspots. *Atmospheric Environment*, 209, 220–232. doi: <https://doi.org/10.1016/j.atmosenv.2019.04.006>
- Massoli, P., Lambe, A. T., Ahern, A. T., Williams, L. R., Ehn, M., Mikkilä, J., Canagaratna, M. R., Brune, W. H., Onasch, T. B., Jayne, J. T., Petäjä, T., Kulmala, M., Laaksonen, A., Kolb, C. E., Davidovits, P., & Worsnop, D. R. (2010). Relationship between aerosol oxidation level and hygroscopic properties of laboratory generated secondary organic aerosol (SOA) particles. *Geophysical Research Letters*, 37(24). doi: <https://doi.org/10.1029/2010GL045258>
- Mirante, F., Salvador, P., Pio, C., Alves, C., Artíñano, B., Caseiro, A., & Revuelta, M. (2014, 03). Size fractionated aerosol composition at roadside and background environments in the Madrid urban atmosphere. *Atmospheric Research*, 138, 278–292. doi: 10.1016/j.atmosres.2013.11.024
- Moore, R. H., & Raymond, T. M. (2008). HTDMA analysis of multicomponent dicarboxylic acid aerosols with comparison to UNIFAC and ZSR. *Journal of Geophysical Research: Atmospheres*, 113(D4). doi: <https://doi.org/10.1029/2007JD008660>
- Mukherjee, S., Singla, V., Pandithurai, G., Safai, P., Meena, G., Dani, K., & Anil Kumar, V. (2018). Seasonal variability in chemical composition and source apportionment of sub-micron aerosol over a high altitude site in Western Ghats, India. *Atmospheric Environment*, 180, 79–92. doi: <https://doi.org/10.1016/j.atmosenv.2018.02.048>
- Murthy, B., Latha, R., Tiwari, A., Rathod, A., Singh, S., & Beig, G. (2020). Impact of mixing layer height on air quality in winter. *Journal of Atmospheric and Solar-Terrestrial Physics*, 197, 105157. doi: <https://doi.org/10.1016/j.jastp.2019.105157>

- Nenes, A., Pandis, S., & Pilinis, C. (1998, 03). ISORROPIA: A New Thermodynamic Equilibrium Model for Multiphase Multicomponent Inorganic Aerosols. *Aquatic Geochemistry*, 4, 123-152. doi: 10.1023/A:1009604003981
- Nguyen, T. K. V., Zhang, Q., Jimenez, J. L., Pike, M., & Carlton, A. G. (2016). Liquid Water: Ubiquitous Contributor to Aerosol Mass. *Environmental Science & Technology Letters*, 3(7), 257-263. doi: 10.1021/acs.estlett.6b00167
- Nuaaman, I., Li, S.-M., Hayden, K., Onasch, T., Sueper, D., Worsnop, D., Bates, T., Quinn, P., & McLaren, R. (2015, 01). Separating refractory and non-refractory particulate chloride and estimating chloride depletion by aerosol mass spectrometry in a marine environment. *Atmospheric Chemistry and Physics Discussions*, 15, 2085-2118. doi: 10.5194/acpd-15-2085-2015
- Ojha, N., Sharma, A., Kumar, M., Imran, G., Ansari, T., Sharma, S., Singh, N., Pozzer, A., & Gunthe, S. S. (2020, 04). On the widespread enhancement in fine particulate matter across the Indo-Gangetic Plain towards winter. *Scientific Reports*, 10. doi: 10.1038/s41598-020-62710-8
- Pandey, A., Brauer, M., Cropper, M. L., Balakrishnan, K., Mathur, P., Dey, S., Turkoglu, B., Kumar, G. A., Khare, M., Beig, G., Gupta, T., Krishnankutty, R. P., Causey, K., Cohen, A. J., Bhargava, S., Aggarwal, A. N., Agrawal, A., Awasthi, S., Bennitt, F., Bhagwat, S., Bhanumati, P., Burkart, K., Chakma, J. K., Chiles, T. C., Chowdhury, S., Christopher, D. J., Dey, S., Fisher, S., Fraumeni, B., Fuller, R., Ghoshal, A. G., Golechha, M. J., Gupta, P. C., Gupta, R., Gupta, R., Gupta, S., Guttikunda, S., Hanrahan, D., Harikrishnan, S., Jeemon, P., Joshi, T. K., Kant, R., Kant, S., Kaur, T., Koul, P. A., Kumar, P., Kumar, R., Larson, S. L., Lodha, R., Madhipatla, K. K., Mahesh, P. A., Malhotra, R., Managi, S., Martin, K., Mathai, M., Mathew, J. L., Mehrotra, R., Mohan, B. V. M., Mohan, V., Mukhopadhyay, S., Mutreja, P., Naik, N., Nair, S., Pandian, J. D., Pant, P., Perianayagam, A., Prabhakaran, D., Prabhakaran, P., Rath, G. K., Ravi, S., Roy, A., Sabde, Y. D., Salvi, S., Sambandam, S., Sharma, B., Sharma, M., Sharma, S., Sharma, R. S., Shrivastava, A., Singh, S., Singh, V., Smith, R., Stanaway, J. D., Taghian, G., Tandon, N., Thakur, J. S., Thomas, N. J., Toteja, G. S., Varghese, C. M., Venkataraman, C., Venugopal, K. N., Walker, K. D., Watson, A. Y., Wozniak, S., Xavier, D., Yadama, G. N., Yadav, G., Shukla, D. K., Bekedam, H. J., Reddy, K. S., Guleria, R., Vos, T., Lim, S. S., Dandona, R., Kumar, S., Kumar, P., Landrigan, P. J., & Dandona, L. (2021). Health and economic impact of air pollution in the states of India: the Global Burden of Disease Study 2019. *The Lancet Planetary Health*, 5(1), e25-e38. doi: [https://doi.org/10.1016/S2542-5196\(20\)30298-9](https://doi.org/10.1016/S2542-5196(20)30298-9)
- Patel, A., & Rastogi, N. (2018). Seasonal variability in chemical composition and oxidative potential of ambient aerosol over a high altitude site in western India. *Science of The Total Environment*, 644, 1268-1276.
- Pathak, R. K., Wu, W. S., & Wang, T. (2009). Summertime PM_{2.5} ionic species in four major cities of China: nitrate formation in an ammonia-deficient atmosphere. *Atmospheric Chemistry and Physics*, 9(5), 1711-1722. doi: 10.5194/acp-9-1711-2009
- Petters, M. D., Carrico, C. M., Kreidenweis, S. M., Prenni, A. J., DeMott, P. J., Collett Jr., J. L., & Moosmüller, H. (2009). Cloud condensation nucleation activity of biomass burning aerosol. *Journal of Geophysical Research: Atmospheres*, 114(D22). doi: <https://doi.org/10.1029/2009JD012353>
- Petters, M. D., & Kreidenweis, S. (2007, 04). A single parameter representation of hygroscopic growth and cloud condensation nuclei activity. *Atmospheric Chemistry and Physics*, 7, 1961-1971. doi: 10.5194/acp-7-1961-2007
- Pilinis, C., & Seinfeld, J. H. (1987). Continued development of a general equilibrium model for inorganic multicomponent atmospheric aerosols. *Atmospheric Environment* (1987), 21(11), 2453-2466. doi: <https://doi.org/10.1016/>

- 0004-6981(87)90380-5
- Ram, K., & Sarin, M. (2011). Day–night variability of EC, OC, WSOC and inorganic ions in urban environment of Indo-Gangetic Plain: Implications to secondary aerosol formation. *Atmospheric Environment*, 45(2), 460-468. doi: <https://doi.org/10.1016/j.atmosenv.2010.09.055>
- Ram, K., Sarin, M. M., & Tripathi, S. N. (2010). A 1 year record of carbonaceous aerosols from an urban site in the Indo-Gangetic Plain: Characterization, sources, and temporal variability. *Journal of Geophysical Research: Atmospheres*, 115(D24). doi: <https://doi.org/10.1029/2010JD014188>
- Rastogi, N., Singh, A., Sarin, M., & Singh, D. (2016). Temporal variability of primary and secondary aerosols over northern India: Impact of biomass burning emissions. *Atmospheric Environment*, 125, 396-403. (South Asian Aerosols And Anthropogenic Emissions: Regional And Global Climate Implications) doi: <https://doi.org/10.1016/j.atmosenv.2015.06.010>
- Rengarajan, R., Sudheer, A., & Sarin, M. (2011, 12). Wintertime PM_{2.5} and PM₁₀ carbonaceous and inorganic constituents from urban site in western India. *Atmospheric Research*, 102, 420–431. doi: [10.1016/j.atmosres.2011.09.005](https://doi.org/10.1016/j.atmosres.2011.09.005)
- Rood, M. J., Covert, D. S., & Larson, T. V. (1987). Hygroscopic properties of atmospheric aerosol in Riverside, California. *Tellus B: Chemical and Physical Meteorology*, 39(4), 383-397. doi: [10.3402/tellusb.v39i4.15357](https://doi.org/10.3402/tellusb.v39i4.15357)
- Rood, M. J., Shaw, M., Larson, T., & Covert, D. (1989, 02). Ubiquitous nature of ambient metastable aerosol. *Nature*, 337, 537-539. doi: [10.1038/337537a0](https://doi.org/10.1038/337537a0)
- Samiksha, S., Kumar, S., & Raman, R. (2021, 04). Two-year record of carbonaceous fraction in ambient PM_{2.5} over a forested location in central India: temporal characteristics and estimation of secondary organic carbon. *Air Quality Atmosphere Health*, 950. doi: [10.1007/s11869-020-00951-2](https://doi.org/10.1007/s11869-020-00951-2)
- Sarin, M., Kumar, A., Bikkina, S., Sudheer, A., & Rastogi, N. (2011, 06). Anthropogenic sulphate aerosols and large Cl-deficit in marine atmospheric boundary layer of tropical Bay of Bengal. *Journal of Atmospheric Chemistry*, 66. doi: [10.1007/s10874-011-9188-z](https://doi.org/10.1007/s10874-011-9188-z)
- Satsangi, A., Mangal, A., Agarwal, A., Lakhani, A., & Kumari, K. M. (2021). Variation of carbonaceous aerosols and water soluble inorganic ions during winter haze in two consecutive years. *Atmospheric Pollution Research*, 12(3), 242-251. doi: <https://doi.org/10.1016/j.apr.2020.12.011>
- Saxena, M., Sharma, A., Sen, A., Saxena, P., Saraswati, Mandal, T., Sharma, S., & Sharma, C. (2017). Water soluble inorganic species of PM₁₀ and PM_{2.5} at an urban site of Delhi, India: Seasonal variability and sources. *Atmospheric Research*, 184, 112-125. doi: <https://doi.org/10.1016/j.atmosres.2016.10.005>
- Saxena, P., Belle Hudischewskyj, A., Seigneur, C., & Seinfeld, J. H. (1986). A comparative study of equilibrium approaches to the chemical characterization of secondary aerosols. *Atmospheric Environment (1967)*, 20(7), 1471-1483. doi: [https://doi.org/10.1016/0004-6981\(86\)90019-3](https://doi.org/10.1016/0004-6981(86)90019-3)
- Saxena, P., Hildemann, L. M., McMurry, P. H., & Seinfeld, J. H. (1995). Organics alter hygroscopic behavior of atmospheric particles. *Journal of Geophysical Research: Atmospheres*, 100(D9), 18755-18770. doi: <https://doi.org/10.1029/95JD01835>
- Schlag, P., Kiendler-Scharr, A., Blom, M. J., Canonaco, F., Henzing, J. S., Moerman, M., Prévôt, A. S. H., & Holzinger, R. (2016). Aerosol source apportionment from 1-year measurements at the CESAR tower in Cabauw, the Netherlands. *Atmospheric Chemistry and Physics*, 16(14), 8831–8847. doi: [10.5194/acp-16-8831-2016](https://doi.org/10.5194/acp-16-8831-2016)
- Seinfeld, J. H., & Pandis, S. N. (2016). *Atmospheric Chemistry and Physics: From Air Pollution to Climate Change* (3rd ed.). New Jersey: Wiley.
- Sequeira, R., & Lai, K.-H. (1998). The effect of meteorological parameters and aerosol constituents on visibility in urban Hong Kong. *Atmospheric Environ-*

- ment, 32(16), 2865-2871. doi: [https://doi.org/10.1016/S1352-2310\(97\)00494-9](https://doi.org/10.1016/S1352-2310(97)00494-9)
- Sharma, M., Kishore, S., Tripathi, S., & Behera, S. (2007, 09). Role of atmospheric ammonia in the formation of inorganic secondary particulate matter: A study at Kanpur, India. *Journal of Atmospheric Chemistry*, 58, 1-17. doi: 10.1007/s10874-007-9074-x
- Sharma, S. K., Kotnala, G., & Mandal, T. (2020, 03). Spatial Variability and Sources of Atmospheric Ammonia in India: A Review. , 4, 1-8. doi: 10.1007/s41810-019-00052-3
- Shen, X., Sun, J., Zhang, X., Zhang, Y., Zhong, J., Wang, X., Wang, Y., & Xia, C. (2019). Variations in submicron aerosol liquid water content and the contribution of chemical components during heavy aerosol pollution episodes in winter in Beijing. *Science of The Total Environment*, 693, 133521. doi: <https://doi.org/10.1016/j.scitotenv.2019.07.327>
- Shrestha, P., Barros, A., & Khlystov, A. (2013, 04). CCN estimates from bulk hygroscopic growth factors of ambient aerosols during the pre-monsoon season over Central Nepal. *Atmospheric Environment*, 67, 120-129. doi: 10.1016/j.atmosenv.2012.10.042
- Singh, S., & Kulshrestha, U. C. (2012). Abundance and distribution of gaseous ammonia and particulate ammonium at Delhi, India. *Biogeosciences*, 9(12), 5023-5029. doi: 10.5194/bg-9-5023-2012
- Song, S., Gao, M., Xu, W., Sun, Y., Worsnop, D. R., Jayne, J. T., Zhang, Y., Zhu, L., Li, M., Zhou, Z., Cheng, C., Lv, Y., Wang, Y., Peng, W., Xu, X., Lin, N., Wang, Y., Wang, S., Munger, J. W., Jacob, D. J., & McElroy, M. B. (2019). Possible heterogeneous chemistry of hydroxymethanesulfonate (HMS) in northern China winter haze. *Atmospheric Chemistry and Physics*, 19(2), 1357-1371. doi: 10.5194/acp-19-1357-2019
- S. Raj, S., Krüger, O. O., Sharma, A., Panda, U., Pöhlker, C., Walter, D., Förster, J.-D., Singh, R. P., S., S., Klimach, T., Darbyshire, E., Martin, S. T., McFiggans, G., Coe, H., Allan, J., R., R., Soni, V. K., Su, H., Andreae, M. O., Pöschl, U., Pöhlker, M. L., & Gunthe, S. S. (2021). Planetary Boundary Layer Height Modulates Aerosol—Water Vapor Interactions During Winter in the Megacity of Delhi. *Journal of Geophysical Research: Atmospheres*, 126(24), e2021JD035681. (e2021JD035681 2021JD035681) doi: <https://doi.org/10.1029/2021JD035681>
- Stockwell, W. R., Watson, J. G., Robinson, N. F., Steiner, W., & Sylte, W. W. (2000). The ammonium nitrate particle equivalent of NO_x emissions for wintertime conditions in Central California's San Joaquin Valley. *Atmospheric Environment*, 34(27), 4711-4717. doi: [https://doi.org/10.1016/S1352-2310\(00\)00148-5](https://doi.org/10.1016/S1352-2310(00)00148-5)
- Stokes, R. H., & Robinson, R. A. (1966). Interactions in Aqueous Non-electrolyte Solutions. I. Solute-Solvent Equilibria. *The Journal of Physical Chemistry*, 70(7), 2126-2131. doi: 10.1021/j100879a010
- Tan, H., Cai, M., Fan, Q., Liu, L., Li, F., Chan, P., Deng, X., & Wu, D. (2017). An analysis of aerosol liquid water content and related impact factors in Pearl River Delta. *Science of The Total Environment*, 579, 1822-1830. doi: <https://doi.org/10.1016/j.scitotenv.2016.11.167>
- Tang, I. N., & Fung, K. H. (1997). Hydration and Raman scattering studies of levitated microparticles: Ba(NO₃)₂, Sr(NO₃)₂, and Ca(NO₃)₂. *The Journal of Chemical Physics*, 106(5), 1653-1660. doi: 10.1063/1.473318
- Tang, I. N., Fung, K. H., Imre, D. G., & Munkelwitz, H. R. (1995). Phase Transformation and Metastability of Hygroscopic Microparticles. *Aerosol Science and Technology*, 23(3), 443-453. doi: 10.1080/02786829508965327
- Tao, J., Gao, J., Zhang, L., Zhang, R., Che, H., Zhang, Z., Lin, Z., Jing, J., Cao, J., & Hsu, S.-C. (2014). PM_{2.5} pollution in a megacity of southwest China: source

- apportionment and implication. *Atmospheric Chemistry and Physics*, 14(16), 8679–8699. doi: 10.5194/acp-14-8679-2014
- Tao, J., Zhang, Z., Zhang, L., Wu, Y., Fang, P., & Wang, B. (2021). Impact of aerosol liquid water content and its size distribution on hygroscopic growth factor in urban Guangzhou of South China. *Science of The Total Environment*, 789, 148055. doi: <https://doi.org/10.1016/j.scitotenv.2021.148055>
- Thamban, N. M., Joshi, B., Tripathi, S. N., Sueper, D., Canagaratna, M. R., Moosakutty, S. P., Satish, R., & Rastogi, N. (2019). Evolution of Aerosol Size and Composition in the Indo-Gangetic Plain: Size-Resolved Analysis of High-Resolution Aerosol Mass Spectra. *ACS Earth and Space Chemistry*, 3(5), 823–832. doi: 10.1021/acsearthspacechem.8b00207
- Turpin, B., & Lim, H.-J. (2001, 07). Species Contributions to PM_{2.5} Mass Concentrations: Revisiting Common Assumptions for Estimating Organic Mass. *Aerosol Science and Technology*, 35, 602–610. doi: 10.1080/02786820152051454
- Wang, G., Zhang, R., Gomez, M. E., Yang, L., Levy Zamora, M., Hu, M., Lin, Y., Peng, J., Guo, S., Meng, J., Li, J., Cheng, C., Hu, T., Ren, Y., Wang, Y., Gao, J., Cao, J., An, Z., Zhou, W., Li, G., Wang, J., Tian, P., Marrero-Ortiz, W., Secret, J., Du, Z., Zheng, J., Shang, D., Zeng, L., Shao, M., Wang, W., Huang, Y., Wang, Y., Zhu, Y., Li, Y., Hu, J., Pan, B., Cai, L., Cheng, Y., Ji, Y., Zhang, F., Rosenfeld, D., Liss, P. S., Duce, R. A., Kolb, C. E., & Molina, M. J. (2016). Persistent sulfate formation from London Fog to Chinese haze. *Proceedings of the National Academy of Sciences*, 113(48), 13630–13635. doi: 10.1073/pnas.1616540113
- Wang, Y., Chen, Y., Wu, Z., Shang, D., Bian, Y., Du, Z., Schmitt, S. H., Su, R., Gkatzelis, G. I., Schlag, P., Hohaus, T., Voliotis, A., Lu, K., Zeng, L., Zhao, C., Alfarra, M. R., McFiggans, G., Wiedensohler, A., Kiendler-Scharr, A., Zhang, Y., & Hu, M. (2020). Mutual promotion between aerosol particle liquid water and particulate nitrate enhancement leads to severe nitrate-dominated particulate matter pollution and low visibility. *Atmospheric Chemistry and Physics*, 20(4), 2161–2175. doi: 10.5194/acp-20-2161-2020
- Wexler, A. S., & Clegg, S. (2002, 07). Atmospheric aerosol models for systems including the ions H⁺, NH₄⁺, Na⁺, SO₄²⁻, NO₃⁻, Cl⁻, Br⁻, and H₂O. *Journal of Geophysical Research*, 107. doi: 10.1029/2001JD000451
- Wexler, A. S., & Seinfeld, J. H. (1991). Second-generation inorganic aerosol model. *Atmospheric Environment. Part A. General Topics*, 25(12), 2731–2748. doi: [https://doi.org/10.1016/0960-1686\(91\)90203-J](https://doi.org/10.1016/0960-1686(91)90203-J)
- Wu, Z., Wang, Y., Tan, T., Zhu, Y., Li, M., Shang, D., Wang, H., Lu, K., Guo, S., Zeng, L., & Zhang, Y. (2018, Mar 13). Aerosol Liquid Water Driven by Anthropogenic Inorganic Salts: Implying Its Key Role in Haze Formation over the North China Plain. *Environmental Science & Technology Letters*, 5(3), 160–166. doi: 10.1021/acs.estlett.8b00021
- Wu, Z. J., Poulain, L., Henning, S., Dieckmann, K., Birmili, W., Merkel, M., van Pinxteren, D., Spindler, G., Müller, K., Stratmann, F., Herrmann, H., & Wiedensohler, A. (2013). Relating particle hygroscopicity and CCN activity to chemical composition during the HCCT-2010 field campaign. *Atmospheric Chemistry and Physics*, 13(16), 7983–7996. doi: 10.5194/acp-13-7983-2013
- Yadav, S., & Kumar, P. (2014). Pollutant scavenging in dew water collected from an urban environment and related implications. *Air Quality Atmosphere Health*, 7, 559–566. doi: 10.1007/s11869-014-0258-7
- Zaveri, R. A., Easter, R. C., & Peters, L. K. (2005). A computationally efficient Multicomponent Equilibrium Solver for Aerosols (MESA). *Journal of Geophysical Research: Atmospheres*, 110(D24). doi: <https://doi.org/10.1029/2004JD005618>
- Zhang, Y., Tang, L., Croteau, P. L., Favez, O., Sun, Y., Canagaratna, M. R., Wang,

- 1407 Z., Couvidat, F., Albinet, A., Zhang, H., Sciare, J., Prévôt, A. S. H., Jayne,
1408 J. T., & Worsnop, D. R. (2017). Field characterization of the PM_{2.5} Aerosol
1409 Chemical Speciation Monitor: insights into the composition, sources, and pro-
1410 cesses of fine particles in eastern China. *Atmospheric Chemistry and Physics*,
1411 *17*(23), 14501–14517. doi: 10.5194/acp-17-14501-2017
- 1412 Zheng, G., Su, H., Wang, S., Andreae, M. O., Pöschl, U., & Cheng, Y. (2020). Mul-
1413 tiphase buffer theory explains contrasts in atmospheric aerosol acidity. *Science*,
1414 *369*(6509), 1374–1377. doi: 10.1126/science.aba3719
- 1415 Örjan Gustafsson, Kruså, M., Zencak, Z., Sheesley, R. J., Granat, L., Engström, E.,
1416 Praveen, P. S., Rao, P. S. P., Leck, C., & Rodhe, H. (2009). Brown Clouds
1417 over South Asia: Biomass or Fossil Fuel Combustion? *Science*, *323*(5913),
1418 495–498. doi: 10.1126/science.1164857

Complex interplay between organic and secondary inorganic aerosols with ambient relative humidity implicates the aerosol liquid water content over India during wintertime”

Amar Krishna Gopinath^{1,2}, Subha S. Raj^{2,3}, Snehitha M. Kommula^{2,3},
Christi Jose^{2,3}, Upasana Panda^{2,3,4}, Yukti Bishambu^{2,3}, Narendra Ojha⁵, R.
Ravikrishna^{1,2}, Pengfei Liu⁶, Sachin S. Gunthe^{2,3}

¹Department of Chemical Engineering, Indian Institute of Technology Madras, Chennai, India

²Laboratory for Atmospheric and Climate Sciences, Indian Institute of Technology Madras, Chennai, India

³EWRE Division, Department of Civil Engineering, Indian Institute of Technology Madras, Chennai, India

⁴Academy of Scientific and Innovative Research (AcSIR), Department of Environment and Sustainability, CSIR – Institute of Minerals and Materials Technology, Bhubaneswar, India

⁵Space and Atmospheric Sciences Division, Physical Research Laboratory, Ahmedabad 380 009, India

⁶School of Earth and Atmospheric Sciences, Georgia Institute of Technology, Atlanta, GA, USA

Pengfei Liupengfei.liu@eas.gatech.edu

Sachin S. Gunthes.gunthe@iitm.ac.in

Contents of this file

1. Tables S1 to S4
2. Figures S1 to S8

literature.

Table S2. Summary of the average chemical composition of atmospheric aerosols at locations across India reported in

Reference	Location	Type	Period	Duration	Mode	Species mass concentration in $\mu\text{g m}^{-3}$ air (mass fraction)						
						NH_4^+	SO_4^{2-}	NO_3^-	Cl^-	OC	Org	K^+
Gani et al. (2019)	New Delhi	Urban	Dec 2017 to Feb 2018	2.5 months	ACSM	20.0 (0.10)	16.0 (0.08)	24.0 (0.12)	23.1 (0.12)	-	112.0 (0.57)	-
Thamban et al. (2019)	Kaampur	Urban	1-31 Jan 2016	1 month	AMS	46.4 (0.11)	52.3 (0.13)	71.2 (0.18)	19.3 (0.05)	-	217.2 (0.053)	-
Kommula et al. (2021)	Chennai	Urban	5 Jan - 1 Feb 2019	1 month	ACSM	3.6 (0.12)	10.1 (0.33)	1.3 (0.04)	0.83 (0.03)	-	14.4 (0.48)	-
Mukherjee et al. (2018)	Mathabaleshwar	Rural	5 Jan- 1 Feb 2019	1 month	ACSM	1.28 (0.10)	3.0 (0.24)	0.96 (0.08)	0.11 (0.01)	-	7.02 (0.57)	-
Kompathi et al. (2020)	Bhubaneswar	Urban	Dec 2016-Feb 2017	3 months	AMS	2.08 (0.10)	5.47 (0.27)	2.1 (0.10)	0.52 (0.03)	-	9.82 (0.49)	-
Ajith et al. (2022)	Thiruvananthapuram	Urban	Winter 2017-2020	-	ACSM	3.45 (0.06)	10.90 (0.20)	1.69 (0.03)	0.24 (0.00)	-	37.5 (0.70)	-
Rastogi et al. (2016)	Patna	Urban	Dec 2011- Feb 2012	3 months	Filter	16.5 (0.12)	24.57 (0.18)	22.34 (0.16)	3.9 (0.03)	42.58	68.13 (0.50)	2.73
Reengrajan et al. (2011)	Ahmedabad	Urban	8 Dec 2006- 7 Jan 2007	1 month	Filter	3.2 (0.07)	9.7 (0.22)	1.2 (0.03)	0.08 (0.00)	18.3	29.28 (0.67)	0.9
S. Kumar and Raman (2016); Samiksha et al. (2021)	Bhopal	Urban	Jan-Feb 2012,2013	2 months	Filter	7.54 (0.09)	23.25 (0.08)	5.99 (0.13)	1.08 (0.03)	31.48	50.37 (0.67)	2.85
S. Kumar et al. (2018)	Amritsar	Urban	Dec 2011- Feb 2012	3months	Filter	4.08 (0.09)	3.95 (0.26)	6.08 (0.07)	1.3 (0.01)	19.56	31.29 (0.57)	0.81
A. Kumar and Saria (2010)	Mount Abu	Rural	Jan-Feb, Oct-Dec 2007	5 months	Filter	1.83	4.98	0.34	0	-	-	-
Agarwal et al. (2020)	Sikandarpur	Rural	Dec-Feb 2015-17	3 months	Filter	13.12	13.25	13.03	13.25	-	-	3.36
A. Kumar et al. (2020)	Patna	Urban	Jan-Feb, Dec	3 months	Filter	6.21	3.73	3.34	0.43	-	-	1.08

..

Table S1. Quantitative parameters used to identify the dominance of NH_4^+ in aerosol chemical composition.

Location	NH_4^+ equivalent fraction	$\text{NH}_4^+/\text{SO}_4^{2-}$
Patiala	0.90	3.55
Ahmedabad	0.72	1.76
Amritsar	0.73	1.73
Bhopal	0.75	5.51
Mount Abu	0.80	1.96
Sikandarpur	0.71	5.28
Patna	0.77	8.88

Table S3. Estimates of κ_{inorg} and overall κ for all locations. The fit parameter R^2 for κ estimates are also shown.

Location	κ_{inorg}	κ_{org}	κ
New Delhi	0.59	0.08	0.28
Kanpur	0.55	0.08	0.28
Chennai	0.37	0.08	0.22
Mahabaleshwar	0.42	0.13	0.24
Bhubhaneshwar	0.33	0.08	0.20
Thiruvananthapuram	0.39	0.08	0.17
Patiala	0.51	0.08	0.28
Ahmedabad	0.41	0.08	0.18
Amritsar	0.36	0.08	0.19
Bhopal	0.58	0.08	0.23

Table S4. Regimes of salt species modelled in ISORROPIA2.1 (considering only NH_4^+)

Regime	$R_{SO_4} = \text{NH}_4^+/\text{SO}_4^{2-}$	Aerosol type	Salt species
(i)	$R_{SO_4} < 1$	Sulphate super rich	H_2SO_4 , NH_4HSO_4
(ii)	$1 \leq R_{SO_4} < 2$	Sulphate rich	NH_4HSO_4 , $(\text{NH}_4)_3\text{H}(\text{SO}_4)_2$, $(\text{NH}_4)_2\text{SO}_4$
(iii)	$R_{SO_4} \geq 2$	Ammonium rich	$(\text{NH}_4)_2\text{SO}_4$, NH_4NO_3 , NH_4Cl

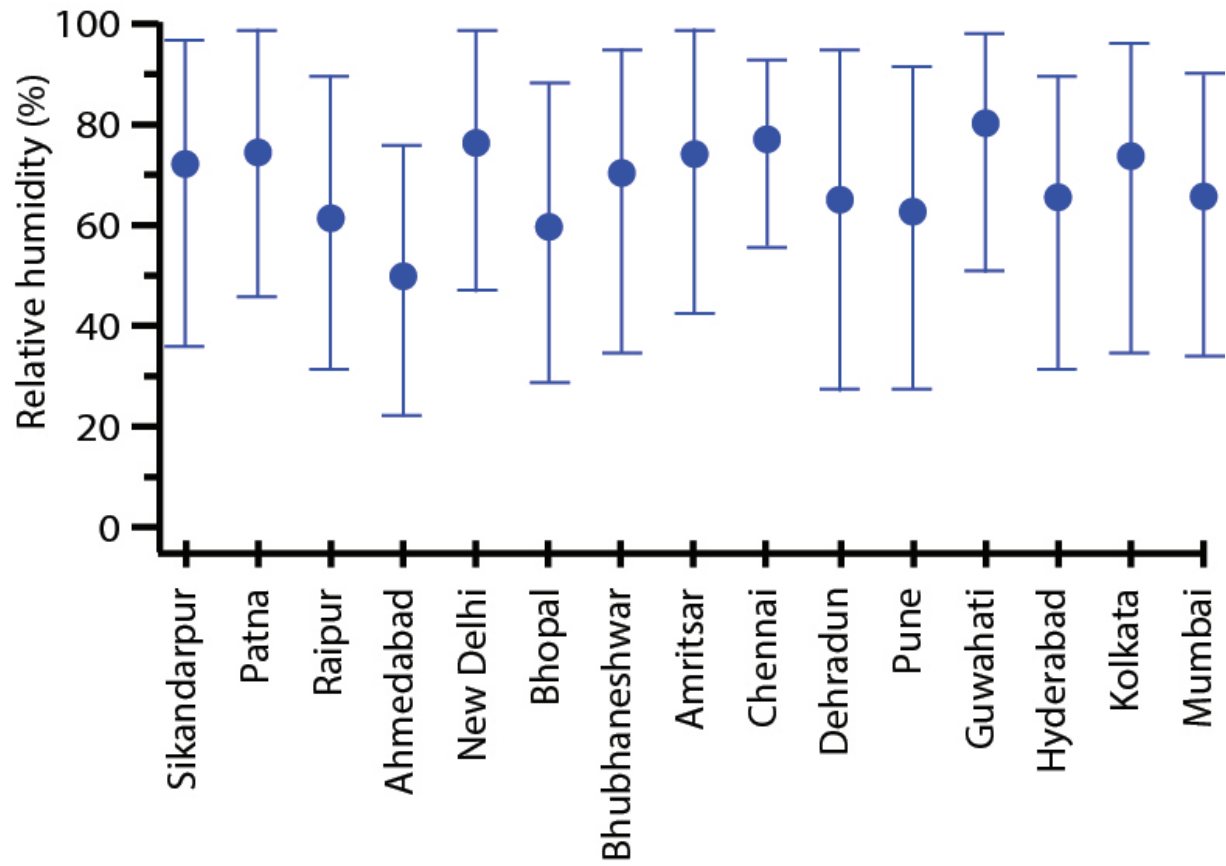


Figure S1. Overview of the atmospheric RH over Indian locations during wintertime. The dots represent the average RH while the whiskers represent the maximum and minimum RH for the corresponding locations.

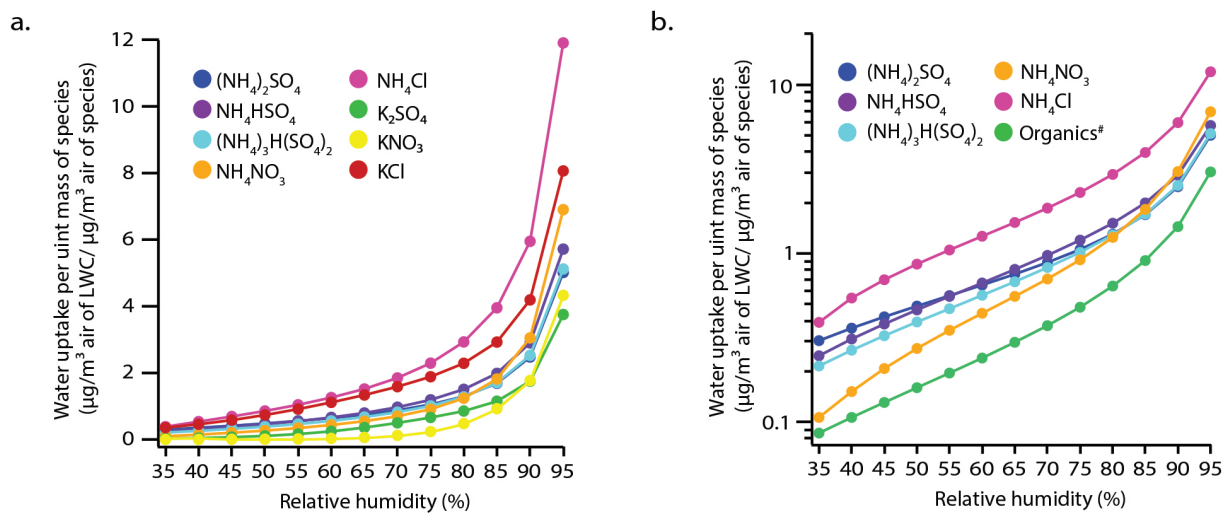


Figure S2. The water uptake per unit mass of species ($\mu\text{g}/\text{m}^3$ air of LWC / $\mu\text{g}/\text{m}^3$ air of species) over a range of RH (35-95%) of (a) major salts of NH_4^+ and K^+ on linear scale (b) major salts of NH_4^+ and organic matter on log scale

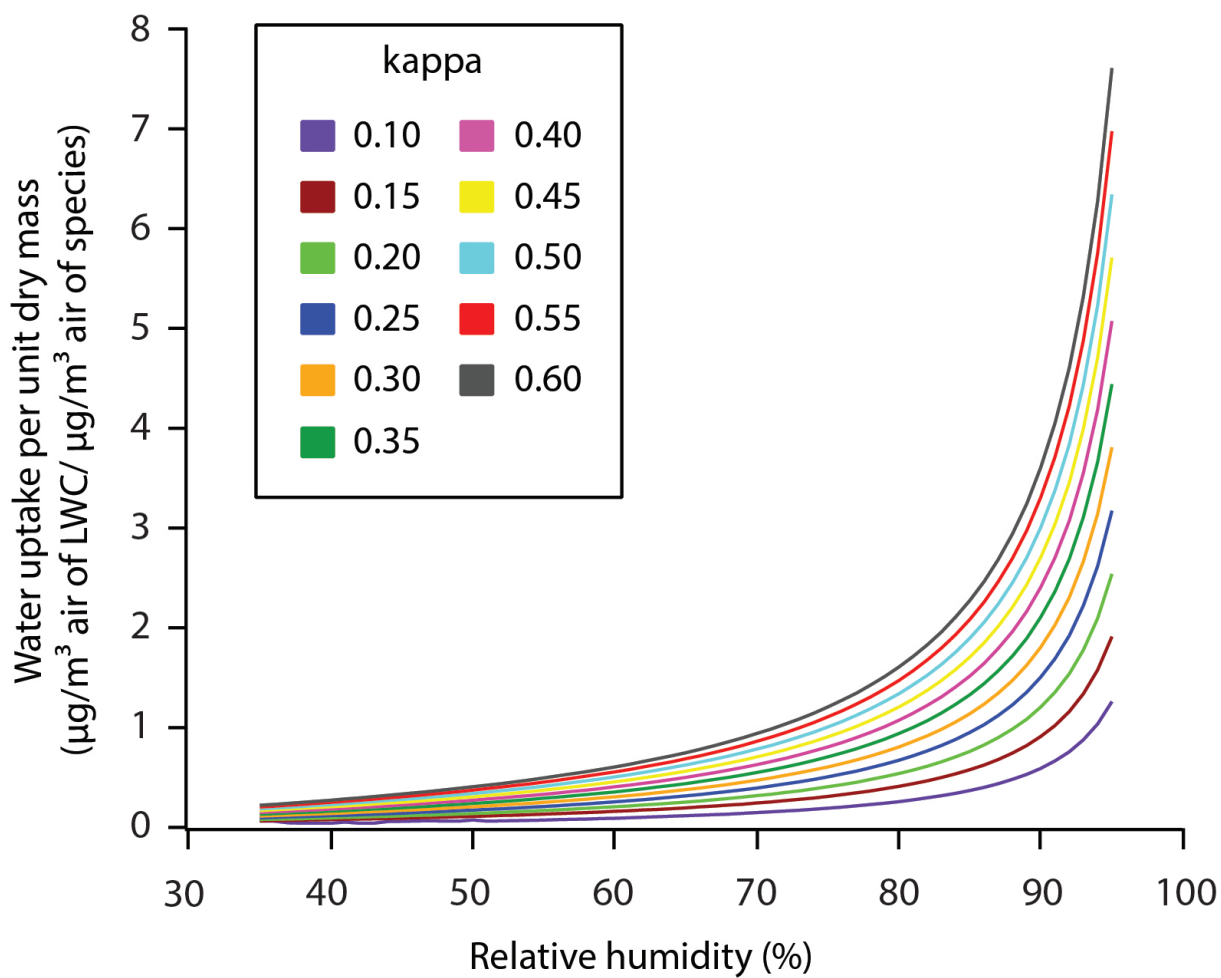


Figure S3. Variation of water uptake per unit dry mass ($\mu\text{g}/\text{m}^3$ air of LWC / $\mu\text{g}/\text{m}^3$ air of species) with RH for κ ranging from 0.1 to 0.6.

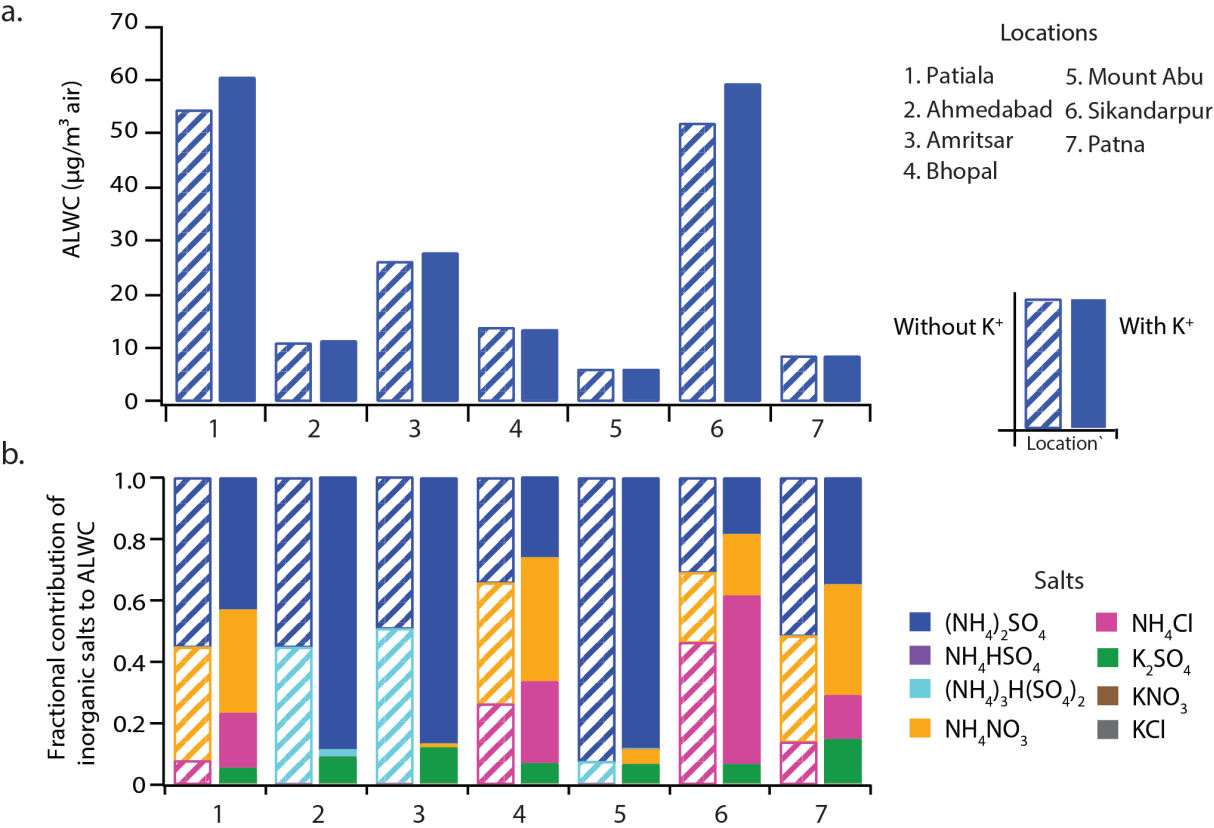


Figure S4. Sensitivity analysis of the effect of including K^+ in the ALWC calculations. For every location, two bars represent data without and with K^+ . (a) Comparison of the absolute ALWC ($\mu\text{g}/\text{m}^3$ air) contributed by inorganic species without and with K^+ . (b) The fractional composition of inorganic species (represented as salts) without and with K^+ .

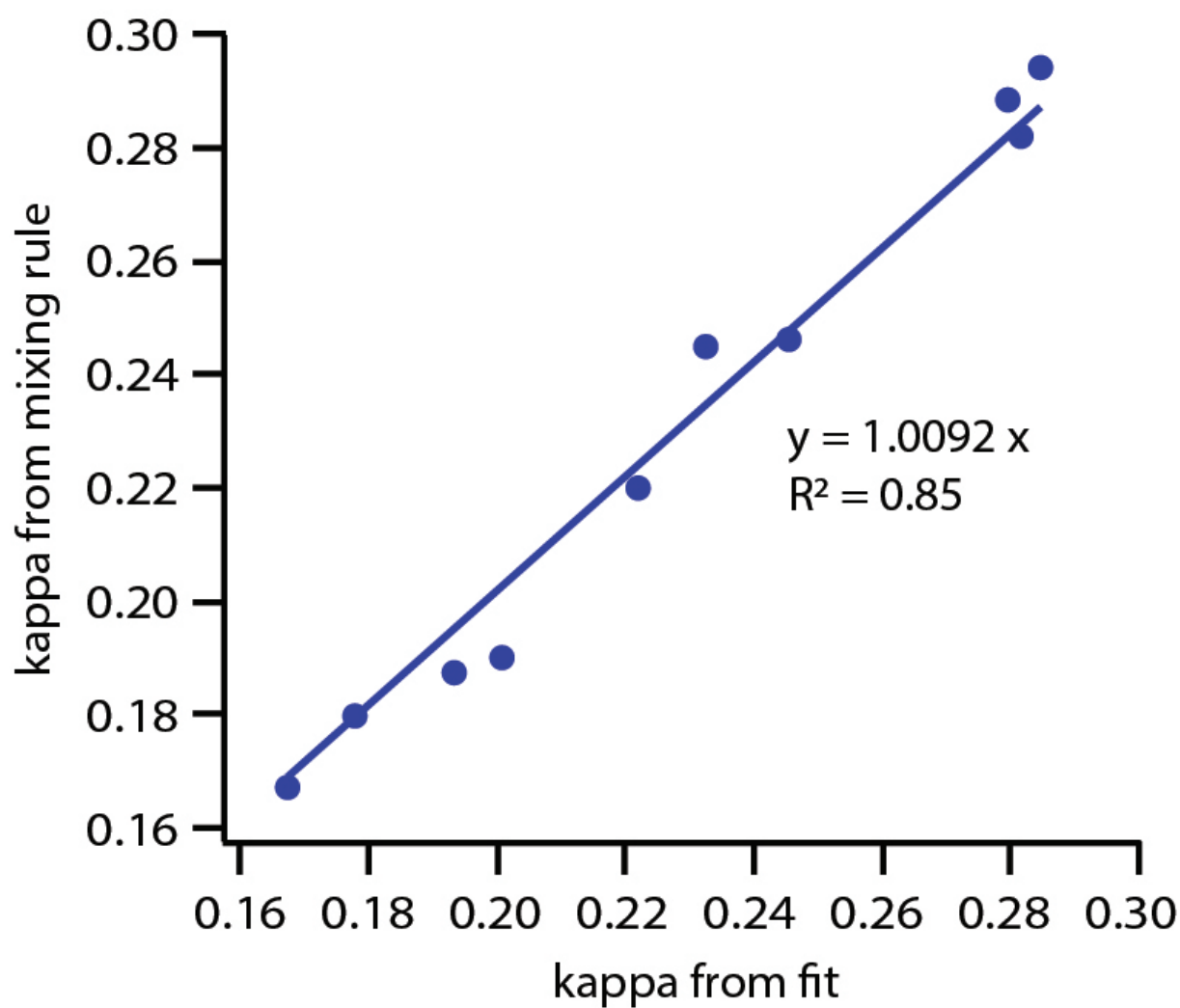


Figure S5. Comparison of the overall kappa from fit with kappa from mixing rule.

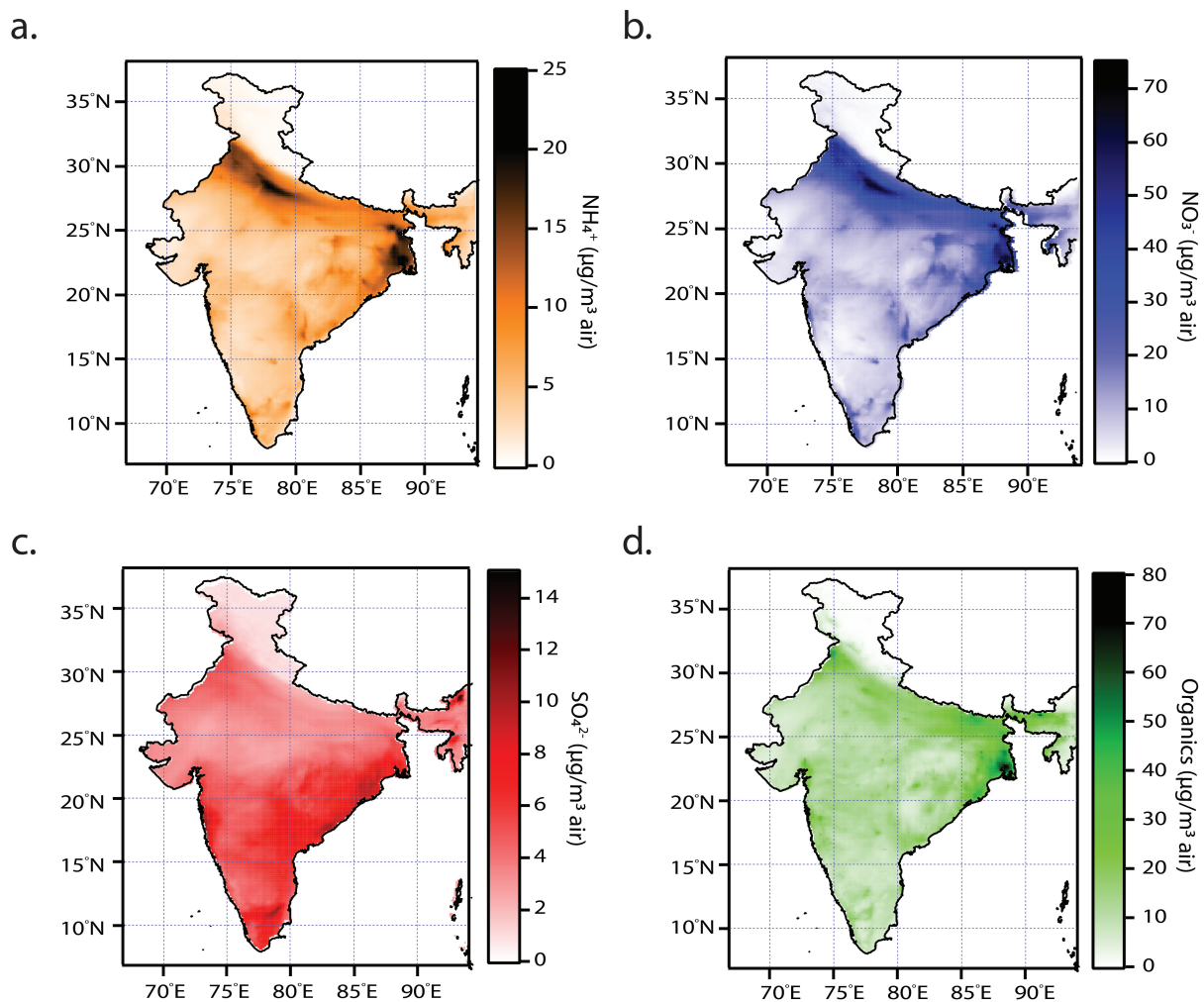


Figure S6. Spatial variation of the mass concentration of the chemical species (a) NH_4^+ (b) NO_3^- , (c) SO_4^{2-} and (d) organic matter over India using data from WRF CHEM model (concentrations in $\mu\text{g}/\text{m}^3$ air).

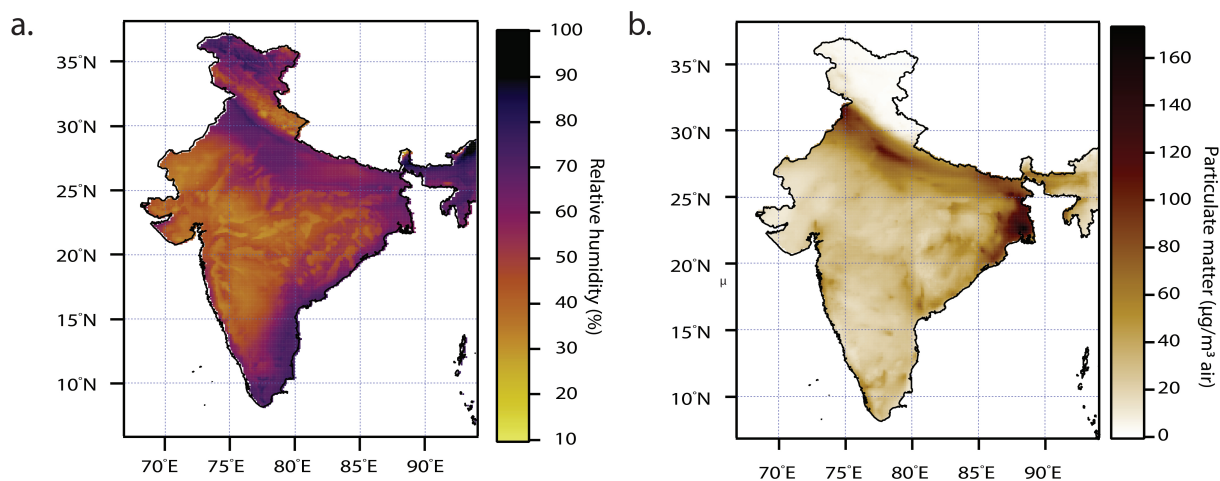


Figure S7. Spatial variation of various parameters calculated from WRF CHEM model for the month of January (a) Relative humidity (%) (b) Total dry aerosol mass ($\mu\text{g}/\text{m}^3$ air).

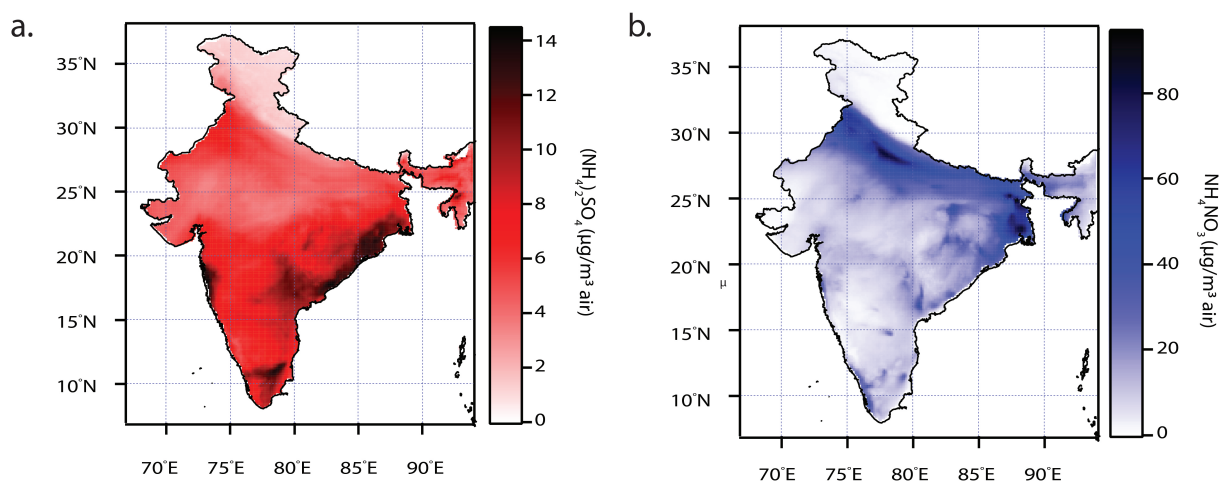


Figure S8. Spatial variation of the mass concentration of the chemical species (a) $(\text{NH}_4)_2\text{SO}_4$ (b) NH_4NO_3 over India predicted by ISORROPIA2.1 using data from WRF CHEM model (concentrations in $\mu\text{g}/\text{m}^3$ air) for the month of January.

References

- Agarwal, A., Satsangi, A., Lakhani, A., & Kumari, K. M. (2020). Seasonal and spatial variability of secondary inorganic aerosols in PM_{2.5} at Agra: Source apportionment through receptor models. *Chemosphere*, 242, 125132. doi: <https://doi.org/10.1016/j.chemosphere.2019.125132>
- Ajith, T., Kompalli, S. K., Nair, V. S., & Babu, S. S. (2022). Mesoscale variations of the chemical composition of submicron aerosols and its influence on the cloud condensation nuclei activation. *Atmospheric Environment*, 268, 118778. doi: <https://doi.org/10.1016/j.atmosenv.2021.118778>

- Gani, S., Bhandari, S., Seraj, S., Wang, D. S., Patel, K., Soni, P., Arub, Z., Habib, G., Hildebrandt Ruiz, L., & Apte, J. S. (2019). Submicron aerosol composition in the world's most polluted megacity: the Delhi Aerosol Supersite study. *Atmospheric Chemistry and Physics*, 19(10), 6843–6859. doi: 10.5194/acp-19-6843-2019
- Kommula, S. M., Upasana, P., Sharma, A., Raj, S. S., Reyes-villegas, E., Liu, T., Allan, J. D., Jose, C., Pöhlker, M. L., Ravikrishna, R., Liu, P., Su, H., Martin, S. T., Pöschl, U., Mcfiggans, G., Coe, H., & Gunthe, S. S. (2021). Chemical Characterization and Source Apportionment of Organic Aerosols in the Coastal City of Chennai, India: Impact of Marine Air Masses on Aerosol Chemical Composition and Potential for Secondary Organic Aerosol Formation. *ACS Earth and Space Chemistry*, 5(11), 3197-3209. doi: 10.1021/acsearthspacechem.1c00276
- Kompalli, S. K., Suresh Babu, S. N., Satheesh, S. K., Krishna Moorthy, K., Das, T., Boopathy, R., Liu, D., Darbyshire, E., Allan, J. D., Brooks, J., Flynn, M. J., & Coe, H. (2020). Seasonal contrast in size distributions and mixing state of black carbon and its association with PM_{1.0} chemical composition from the eastern coast of India. *Atmospheric Chemistry and Physics*, 20(6), 3965–3985. doi: 10.5194/acp-20-3965-2020
- Kumar, A., & Sarin, M. (2010). Atmospheric water-soluble constituents in fine and coarse mode aerosols from high-altitude site in western India: Long-range transport and seasonal variability. *Atmospheric Environment*, 44(10), 1245-1254. doi: <https://doi.org/10.1016/j.atmosenv.2009.12.035>
- Kumar, A., Yadav, I., Shukla, A., & Devi, N. (2020, 08). Seasonal Variation of PM_{2.5} in the Central Indo-Gangetic Plain (Patna) of India: Chemical Characterization and Source Assessment. *Journal of Applied Sciences*. doi: 10.1007/s42452-020-3160-y

- Kumar, S., Nath, S., Bhatti, M., & Yadav, S. (2018, 06). Chemical Characteristics of Fine and Coarse Particles during Winter Time over Two Urban Cities in North India. *Aerosol and Air Quality Research*, 18. doi: 10.4209/aaqr.2018.02.0051
- Kumar, S., & Raman, R. (2016, 08). Inorganic ions in ambient fine particles over a National Park in central India: Seasonality, dependencies between SO₄²⁻, NO₃⁻, and NH₄⁺, and neutralization of aerosol acidity. *Atmospheric Environment*, 143. doi: 10.1016/j.atmosenv.2016.08.037
- Mukherjee, S., Singla, V., Pandithurai, G., Safai, P., Meena, G., Dani, K., & Anil Kumar, V. (2018). Seasonal variability in chemical composition and source apportionment of sub-micron aerosol over a high altitude site in Western Ghats, India. *Atmospheric Environment*, 180, 79-92. doi: <https://doi.org/10.1016/j.atmosenv.2018.02.048>
- Rastogi, N., Singh, A., Sarin, M., & Singh, D. (2016). Temporal variability of primary and secondary aerosols over northern India: Impact of biomass burning emissions. *Atmospheric Environment*, 125, 396-403. (South Asian Aerosols And Anthropogenic Emissions: Regional And Global Climate Implications) doi: <https://doi.org/10.1016/j.atmosenv.2015.06.010>
- Rengarajan, R., Sudheer, A., & Sarin, M. (2011). Wintertime PM_{2.5} and PM₁₀ carbonaceous and inorganic constituents from urban site in western India. *Atmospheric Research*, 102(4), 420-431. doi: <https://doi.org/10.1016/j.atmosres.2011.09.005>
- Samiksha, S., Kumar, S., & Raman, R. (2021, 04). Two-year record of carbonaceous fraction in ambient PM_{2.5} over a forested location in central India: temporal characteristics and estimation of secondary organic carbon. *Air Quality Atmosphere Health*, 950. doi: 10.1007/s11869-020-00951-2
- Thamban, N. M., Joshi, B., Tripathi, S. N., Sueper, D., Canagaratna, M. R., Moosakutty,

S. P., Satish, R., & Rastogi, N. (2019). Evolution of Aerosol Size and Composition in the Indo-Gangetic Plain: Size-Resolved Analysis of High-Resolution Aerosol Mass Spectra. *ACS Earth and Space Chemistry*, 3(5), 823-832. doi: 10.1021/acsearthspacechem.8b00207